

**DISPATCH CAPACITY FORECASTING OF DISTRIBUTED ENERGY  
RESOURCES FOR LOAD PEAK SHAVING**

by

Manuel Arturo Mendoza Miranda

Bachelor of Science, Universidad Central “Marta Abreu” de Las Villas, 2017

A Thesis Submitted in Partial Fulfillment  
of the Requirements for the Degree of

**Master of Science**

in the Graduate Academic Unit of Electrical and Computer Engineering

Supervisor(s): Eduardo Castillo Guerra, PhD, Electrical and Computer Engineering  
Julian Cardenas Barrera, PhD, Electrical and Computer Engineering

Examining Board: Chris Rouse, PhD, Electrical and Computer Engineering  
Julian Meng, PhD, Electrical and Computer Engineering  
Wei Song, PhD, Computer Science

This thesis is accepted by the  
Dean of Graduate Studies

THE UNIVERSITY OF NEW BRUNSWICK

April, 2022

©Manuel Arturo Mendoza Miranda, 2022

## **ABSTRACT**

The progress of the electric power grid to a decentralized and ‘smart’ system has enabled the participation of distributed energy resources (DERs) to provide peak load shaving and ancillary services. This thesis focuses on a probabilistic dispatch capacity forecast of aggregated DERs, with models that allow the simulation of individual loads and the estimation of their potential load shifting capacity during peak hours, while tracking customer comfort. As part of the forecasting method, this work proposes a scheme for aggregated DER control that consists of a modified direct load control strategy and a modified advanced demand response control schedule. The simulation results show the potential of the proposed approach to increase the dispatchable capacity during peak hours in aggregations of the DERs considered, while maintaining customer comfort.

# **DEDICATION**

To my parents and brother.

## ACKNOWLEDGEMENTS

Throughout the writing of this dissertation, I have received a great deal of support and assistance.

First and foremost, I must thank my research supervisors, Dr. Eduardo Castillo Guerra and Dr. Julian Cardenas Barrera, whose knowledge was invaluable in preparing the research questions and methodology. Their insightful feedback pushed me to improve my thinking and prepared me for my future career. Without their assistance this dissertation would never have been accomplished. I would like to deeply thank them for their support, friendship, and patience over these past two years.

A sincere thanks to Dr. Ahmad Mezher for his aid in my dissertation and outside the academia too. He is very knowledgeable and professional, and a great friend as well.

I would like to thank Dr. Julian Meng, who provided insights and feedback on my research and for his great *Digital Image Processing* course, where I acquired tools and knowledge that helped my research.

I wish to express my sincere thanks to Iroel Miranda Castaneda and Taidy Diaz Guerra for their guidance and friendship during the research.

I am also grateful to Dr. Xun Gong for sharing his expertise in the field of my research.

I would like to show my gratitude to Alimohammad Shafieisarves, Zehan Irani and Ismail Mohamed Ali Arafat for their help, brainstorming on the research and their friendship.

Getting through my dissertation required more than academic support. I have many people to thank for listening and tolerating me over the past years. I cannot begin to express my

appreciation for their friendship. Haydée Etelvina Sainz has been an immense influence in the completion of this dissertation. She opened both her home and heart to me when I arrived in the city. I have nothing but the utmost respect for her.

I must express my intense appreciation to my parents and to my brother for providing me with constant support and continuous encouragement throughout the process of researching and writing this thesis. This achievement would not have been possible without them.

Finally, I would like to thank everyone who helped me directly or indirectly in this venture.

# Table of Contents

ABSTRACT.....	ii
DEDICATION.....	ii
ACKNOWLEDGEMENTS.....	iii
Table of Contents.....	v
List of Tables.....	viii
List of Figures.....	ix
List of Symbols, Nomenclature or Abbreviations.....	xii
1 Introduction.....	1
1.1 Motivation.....	1
1.2 Problem Statement.....	4
1.2.1 Aggregated DER Demand Forecast.....	6
1.2.2 Aggregated DER Control and Dispatch Capacity Forecast.....	7
1.3 Objectives.....	8
1.4 Contributions.....	8
1.5 Outline of the Thesis.....	9
2 Literature Review.....	10
2.1 Aggregated DER Demand Forecast.....	10
2.2 Aggregated DER Control.....	13
2.3 Research Gaps.....	14
3 Research Methodology.....	16

3.1	Framework .....	17
3.1.1	The Saint John Local Distribution Network (SJE’s LDN) .....	17
3.2	DER representation .....	17
3.2.1	DEWHs .....	18
3.2.2	Electric baseboard heaters (EBHs) .....	18
3.2.3	Electric Thermal Storage (ETS) systems .....	19
3.3	Aggregation strategy .....	19
3.4	Control algorithms.....	19
3.5	Forecasting algorithm.....	21
3.6	Experimental design.....	21
3.7	End-user comfort evaluation .....	22
3.8	Chapter Conclusions .....	23
4	Aggregate DER Demand Forecast.....	25
4.1	Domestic Electric Water Heaters (DEWHs).....	25
4.1.1	Modelling of DEWHs .....	25
4.1.2	Hot Water Usage Model .....	27
4.1.3	Diversified demand of DEWHs .....	31
4.2	Electric Baseboard Heaters (EBHs) .....	32
4.2.1	Modelling of EBH.....	32
4.2.2	Diversified demand of EBHs .....	34

4.3	Electric Thermal Storage (ETS).....	38
4.3.1	Modelling of ETSS.....	38
4.3.2	Diversified demand of ETSS.....	41
4.4	Chapter Conclusions .....	41
5	Aggregate DER Control and Dispatch Capacity Forecast.....	43
5.1	Direct Temperature Feedback Control.....	43
5.2	Advanced DR setpoint control.....	46
5.3	Dispatch capacity forecast of DEWHs.....	48
5.3.1	Dispatch capacity estimation of aggregated DEWHs.....	53
5.4	Dispatch capacity estimation of aggregated EBHs .....	55
5.5	Dispatch capacity estimation of aggregated ETSS .....	57
5.6	Planning tool .....	59
5.7	Chapter Conclusions .....	60
6	Conclusions and Future Work .....	62
6.1	Future Work .....	64
	Bibliography .....	65
	Curriculum Vitae	

## List of Tables

Table 4.1: Parameters of DEWHs.....	27
Table 4.2: Parameters of EBHs and rooms. ....	35
Table 5.1: DEWHs subsets. ....	44

## List of Figures

Figure 4.1: Temperature of water in the tank with no water usage. ....	26
Figure 4.2: Monthly mains water temperatures and <i>Fmix</i> values using TMY data for Saint John, NB. ....	29
Figure 4.3: Left: Distribution of population vs. occupants. Right: Box plot of liters of hot water usage per day vs. number of occupants.....	30
Figure 4.4: Hot water draw event probability distributions.....	30
Figure 4.5: Average daily hot water consumption profile. ....	31
Figure 4.6: Simulated aggregate water draw for 2000 DEWHs over 24 hours and the corresponding total power demand of the population (autonomous demand).....	32
Figure 4.7: RC network for a room with an EBH.....	33
Figure 4.8: Room temperature with one EBH and a constant outdoor temperature of 0°C. ....	34
Figure 4.9: Power rating distribution of EBHs. ....	36
Figure 4.10: Left: Distribution of pick-up and setback hours. Right: Distribution of temperature differences between setback and setpoint.....	37
Figure 4.11: Outdoor temperature and corresponding autonomous demand of 200 EBHs. ....	37
Figure 4.12: Electric Thermal Storage [87]. ....	38
Figure 4.13: Simplified model of ETS.....	39
Figure 4.14: Bricks' temperature in an ETS with a constant outdoor temperature of 0°C. ....	40
Figure 4.15: Outdoor temperature and corresponding autonomous demand of 50 ETSs. ....	41

Figure 5.1: Rules used to create the setpoint control schedule. ....	47
Figure 5.2: Left: DR schedule designed to a constant customer schedule. Right: DR adapted to a dynamic customer schedule.....	48
Figure 5.3: Comparison between the aggregate power demand of 4000 DEWHs with and without pre-heat period. ....	49
Figure 5.4: DLC strategy. ....	50
Figure 5.5: Aggregate power demand of 2000 DEWHs with DLC program over 24 hours. Top: DLC with minimum water temperature threshold as defined in equation. (5.16). Bottom: DLC with minimum threshold of 50°C during peak period. ....	52
Figure 5.6: Percentage of events in supply temperatures for 2000 DEWHs to deliver hot water under DLC program for 24 hours. Left: DLC with minimum water temperature threshold as defined in equation. (5.16). Right: DLC with minimum threshold of 50°C during peak period. ....	52
Figure 5.7: Probabilistic forecast of the regulated power of 2000 DEWHs. Left: DLC with minimum water temperature threshold as defined in equation. (5.16). Right: DLC with minimum threshold of 50°C during peak period. ....	54
Figure 5.8: Energy capacity of 2000 DEWHs with DLC program. Left: DLC with minimum water temperature threshold as defined in equation. (5.16) ( $x = -2.389$ MWh, $Sx = 0.0633$ MWh, $E = 0.519\%$ ). Right: DLC with minimum threshold of 50°C during peak period ( $x = -3.21$ MWh, $Sx = 0.1896$ MWh, $E = 1.157\%$ ).....	54
Figure 5.9: Aggregate power demand of 200 EBHs with DR schedule over 24 hours. ....	55
Figure 5.10: Percentage of room temperatures deviation from thermostats setpoints.....	55
Figure 5.11: Outdoor temperature range.....	56

Figure 5.12: Left: Probabilistic forecast of the regulated power of 200 EBHs. Right: Energy capacity ( $x = -0.245$ MWh, $Sx = 0.0044$ MWh, $E = 0.39\%$ ).....	57
Figure 5.13: Aggregate power demand of 50 ETSs with DLC over 24 hours.....	58
Figure 5.14: Duration for which the bricks temperature is below the minimum threshold. ....	58
Figure 5.15: Left: Probabilistic forecast of the regulated power of 50 ETSs. Right: Energy capacity ( $x = -0.08$ MWh, $Sx = 0.021$ MWh, $E = 4.76\%$ ).....	59
Figure 5.16: User interface using MATLAB showing an iteration result of the power consumption for an aggregation of 1000 DEWHs.....	60
Figure 5.17: User interface and probabilistic dispatch capacity forecast results for an aggregation of 1000 DEWHs.....	60

## **List of Symbols, Nomenclature or Abbreviations**

BSS	Battery Storage System
DSM	Demand Side Management
DR	Demand Response
ILC	Indirect Load Control
DLC	Direct Load Control
TOU	Time of Use
DEWH	Domestic Electric Water Heater
VPP	Virtual Power Plan
SJE	Saint John Energy
NSERC	Natural Sciences and Engineering Research Council
LDN	Local Distribution Network
DER	Distributed Energy Resource
TCL	Thermostatically Controlled Load
HVAC	Heating Ventilation and Air Conditioning
VSTLF	Very-short Term Load Forecast
MTLF	Medium Term Load Forecast
LTLF	Long Term Load Forecast
ARMA	Autoregressive and Moving Average
NN	Neural Network
HLF	Hierarchical Load Forecast

PLF	Probabilistic Load Forecast
EBH	Electric Baseboard Heater
ETS	Electric Thermal Storage System
MBC	Model-Based Controller
MC	Monte Carlo
DTFC	Direct Temperature Feedback Control
ASHRAE	American Society of Heating Refrigerating and Air-Conditioning Engineers
PMV	Predicted Mean Vote
RC	Resistance-Capacitance

# 1 Introduction

## 1.1 Motivation

Electric energy consumption increases steadily every year as a result of the natural growth of the population [1] and more loads are added to the grid. This is accentuated in fast developing countries where the average amount of electricity consumed per person has also increased [1]. Generation is often sized appropriately to account for this growth. However, the crucial balance between demand and supply is challenged by the penetration of renewable energy sources [2] and electric vehicles [3].

The balance between generation and consumption is necessary to maintain an efficient and economical power system. A severe imbalance can produce system breakdown, particularly in small-inertia grids [4]. Renewable sources such as wind and solar cause uncertain generation variation that challenges the stability of the power grid. The penetration of electric vehicles can also add new stress to the network if not carefully planned [5]. This imbalance is often mitigated through conventional generation dispatch and reserve systems, though activating supplementary power generation tends to be costly [6]. Additional generation sources, like battery storage systems (BSS) can also be deployed to improve system stability, but they are very expensive [4]. An economic and attractive alternative is to control the demand. With an adequate management, the demand can become a flexible resource in developing and advanced economies, as well as in emerging markets. Demand management and BSS are expected to meet almost a quarter of flexibility needs globally by 2030 [7].

The concept of controlling the demand is integral to the “smart grid” paradigm. Although there is no unified definition of “smart grid” [8], all classifications agree that the smart grid is a “dynamically interactive real-time infrastructure” [8] that benefits both consumers and stakeholders [9].

Demand Side Management (DSM) includes everything that is done in the demand side, from a simple light bulb upgrade to the implementation of a complex load management program [10]. DSM is not a new idea; it was introduced by Electric Power Research Institute in 1980s [11] and it has been the subject of research in studies, pilot projects [12] and deployments [13]–[15]. Load management, energy efficiency, and energy savings are some of the main activities associated with DSM. For instance, DSM can be applied to absorb the excess in renewable energy generation like wind in periods of low demand and reduce the amount of fuel burned in power plants [16].

DSM can be used not only to keep the demand balanced with the available generation, but to reduce power consumption peaks. This would reduce the need for generation capacity and therefore, increase the utilization and efficiency of generation investment [16]. There are various categories in DSM, depending on the response timing and the impact in the customers electric usage: Energy Efficiency [17], [18], Time-of-Use [19], [20], Demand Response [10], [21], and Spinning Reserve [10], [18]. Demand response (DR) has a quick response time and a direct or indirect control over the loads [10]. DR is more related with short-term impacts in the electricity market, although it still contributes to the long-term benefits of DSM. Peak shaving refers to the reduction of power to avoid spikes in consumption during short periods [13]. On the other hand, load shifting reduces the

electricity consumption and shift it to an earlier or later time when power prices or grid demand is lower [13].

DR refers to changes in the electric usage by customers from their normal consumption patterns [10]. These changes depend on the type of response the system requires, like limiting the demand during peak periods; shifting their load to a different time; or using locally generated energy. Although DR programs are often implemented to provide load curtailment, they also support demand increase in periods of high supply and low consumption [10].

DR can be achieved through indirect load control (ILC) or direct load control (DLC). ILC is usually accomplished by Time-of-Use (TOU) pricing strategies and does not involve any active control over the customers appliances [22]. TOU rates are designed so the price of electricity is higher during peak periods and lower during off-peak periods. This setting encourages customers to modify their consumption patterns to reduce their electric bill. Although there are pricing schemes that involve real-time pricing in conjunction with programmable thermostats that respond automatically to price signals, this type of control is not adequate for power balance in more complex scenarios [23]. DLC on the other hand, assumes that the loads are under complete control [24]. The customers' devices are controlled remotely by a third party or distribution system operator. The operator has a precise control over the loads, including on/off commands and setpoint signals. Thus, DLC has received large attention in DR programs [25]–[29].

Appliances such as domestic electric water heaters (DEWHs), air-conditioning and space heating units have gained the focus of DLC programs to provide ancillary services due to

their large contribution to peak load demands and their fast response times [30]. DEWHs represent approximately 20% of the total electricity consumption in the Canadian residential sector while 60% of the electricity is used for space heating and cooling [31]. These loads, when aggregated, represent a substantial “virtual storage” that can participate on power markets and compete with traditional electric storage [10]. This aggregation can act as a stand-alone virtual power plant (VPP) or in combination with small generation units (regularly renewable sources).

A load aggregator cannot generate power, it can only store energy. As with any VPP, the most crucial factor is the guaranteed availability [10]. This means that the VPP (or aggregator) must be able to deliver the regulated power as requested by the grid operator. However, residential loads exhibit stochastic power demands [10], making it difficult to forecast their future demand. They might be at a state that cannot be modified by the controller to avoid customer discomfort [32]. The power demand of aggregated loads is more predictable when the aggregation size is large, but uncertainties increase as the aggregation size decreases. Forecast methods need to account for these uncertainties to provide reliable forecasts to the system operator.

## **1.2 Problem Statement**

This thesis was developed at the University of New Brunswick as part of the Saint John Energy's (SJE) smart grid project funded by NSERC. Saint John is a city in the Canadian province of New Brunswick, located on the eastern Atlantic coast. SJE's local distribution network (LDN) supplies electricity to more than 36,500 residents with the help of NB Power, its wholesale energy provider.

The use of electricity in New Brunswick is seasonal and very weather dependent. This produces a dramatic difference in summer and winter loads, where the winter peak doubles the average load of summer [33]. The power grid must be able to supply the highest demand in winter (about 3100 MW province-wide) for only a few days of the year. Thus, NB Power requires to add more expensive and less clean generation to satisfy SJE's power demands for the coldest days, which in turn affects SJE's revenue and customer prices [33].

SJE is introducing distributed energy resources (DERs) to support peak shaving and increase system efficiency. DER refers to a small-scale generation or storage system that operates close to the point of delivery and connects to the grid at the distribution level. DERs include solar panels, electric vehicles, and controllable loads with some sort of energy storage capability, such as thermostatically controlled loads (TCLs). SJE is offering property owners and businesses the opportunity to participate in the smart grid project by renting DERs [34]. Electric vehicle charging stations, residential battery storage devices, baseboard heaters, and residential mini-split heat pumps are among the DERs that SJE intends to integrate into its DR programs [34]. Intelligent DR programs will be implemented to achieve load reduction during peak periods. This can potentially avoid investments in new power plants to meet peak demands and the purchase of expensive peak power on the energy spot markets [33]. It also has the added benefit of reducing greenhouse gas emissions (from oil, coal, and gas-fired generating stations).

The amount of power that can be reduced with aggregated DERs will be referred as dispatch capacity [35] of the aggregation. Only the downward capacity during peak period is considered in this study. The system operator can then manage this capacity to participate

in energy markets and provide ancillary services. This thesis aims at forecasting the aggregated dispatch capacity of different DERs that are involved in Saint John Energy's DR programs.

### **1.2.1 Aggregated DER Demand Forecast**

The forecast of aggregated DERs power demand is an arduous task. The size of the aggregation plays a key role. The load forecast of a small aggregation is affected by the stochastic nature of individual devices' demands more than that of larger aggregations. However, including more devices to an aggregation could be less realistic in the short-term, as it maximum would require bigger investments and more customer involvement in DLC programs. The type of DER also determines the nature of the aggregator and therefore, it influences the predictors to use by the forecasting algorithm. The power consumption of electric water heaters, for instance, is not as correlated with the outdoor temperature as the load demand of an electric baseboard heater. The selection of the best predictors is not a simple task, a detailed assessment needs to be conducted for the specific composition of the aggregator.

Real measurements are unquestionably important to produce accurate forecasts. Historical data of individual loads, including knowledge about device configurations are valuable for DR and DLC in particular [36]. However, gathering this information requires the installation of a large sensing infrastructure with more demanding communications requirements. The sensing and communication scenario rises data privacy and network congestion concerns which also must be addressed [12]. The limited access to real data is often overcome employing mathematical models [37]. These models are usually well

suitable for simulations of large aggregations and are employed in a safe and economic pre-deployment phase, before investing in real devices [20], [38], [39].

Several load forecasting algorithms and methods are reported in literature. The forecasting approach varies mainly according to the time horizon and the stochastic or deterministic technique used, among other characteristics. The use of probabilistic forecasting represents an alternative to the absence of real measurements.

### **1.2.2 Aggregated DER Control and Dispatch Capacity Forecast**

The objective of controlling DERs for peak load management is to maximize the dispatch capacity of the different DERs during peak hours. However, various challenges may prevent attaining this goal:

- **Lack of sensor data:** The limitations of the sensing infrastructure restrict the amount of collected information and affect the estimation of the state of charge of aggregated DERs. Data of individual devices is not always available, adding uncertainties on the effect of the control over user comfort as the exact state of the device is unknown. If users experience serious discomfort, they could withdraw from the program.
- **Local control conflicts:** The autonomous local control of individual devices can override the control commands sent by the operator whenever the comfort and/or the safety of the user are at risk. The local control can then limit the capacity of the DER in DLC. For this reason, there must be an agreement between the operator and the customers to set the limits of the control.

- **Impact of system uncertainties:** The heterogeneous parameters of the devices, time-varying ambient temperatures, random user behavior and limited sensing infrastructure challenge the modeling of DER aggregation and the corresponding dispatch capacity forecast. A probabilistic forecast is utilized to merge the impact of such uncertain environments [40], [41].

### 1.3 Objectives

The previously stated problems motivated us to propose an approach to forecast the dispatch capacity of the aggregation of the DERs relevant to the SJE DR initiative. This approach is based on the hypothesis that shifting the power demand of individual loads can increase the available aggregated dispatchable capacity without affecting customer comfort. This work addresses two specific objectives:

- **DER forecast:** Design and evaluate a short-term probabilistic forecasting method for diverse types of aggregated DERs.
- **DER control:** Implement a control strategy to reduce the demand during peak hours while having a minor impact on customers' comfort.

### 1.4 Contributions

The contributions of this thesis are:

1. The proposed dispatch capacity forecasting, including power consumption forecasting and control of DER aggregators.
  - a. The forecasted capacity of the different DERs can be used by SJE to plan a smart load curtailment and minimize the total load demand peak.

2. The control strategy for aggregated DER control, consisting of a modified DLC strategy and modified advanced DR setpoint control schedule.
  - a. **Modified DLC strategy:** Preheating to the highest temperature limit and increasing the reference power above the autonomous demand and setting the reference power to zero during peak periods.
  - b. **Modified advanced DR setpoint control schedule:** Extension of the decrease interval to cover all the peak period and addition of random delay to the pick-up ramp at the end of peak period.
3. The creation of a planning tool that allows to forecast the dispatch capacity of homogeneous aggregators implemented with DEWHs, electric baseboard heaters and electric thermal storage systems.

## 1.5 Outline of the Thesis

The thesis is organized as follows: Chapter 2 presents a comprehensive literature review and layouts the foundations on existing DER forecasting and control methods. Chapter 3 describes the research methodology followed in this work and the experimental design. Chapter 4 focuses on implemented DERs models, the forecasted demand of their aggregation, and the control algorithms used to shift their demand to non-peak hours. Chapter 5 illustrates the performance of the dispatch capacity forecasting method proposed and the implementation of a planning tool. Finally, Chapter 6 summarizes the conclusions of the thesis work and proposes future directions of this research.

## 2 Literature Review

### 2.1 Aggregated DER Demand Forecast

The electric power industry has been interested in load forecasts for over a century. Load forecasting conventionally indicates predicting future electricity demand at aggregated levels [42]. Forecasting the electricity demand aids businesses to plan and operate their systems in an efficient manner. The use of DSM and the deregulation of the power grid enables residential, commercial, or institutional energy resources to actively participate in the electric grid system. For instance, the research published by Shad et, al [43] forecasted the aggregated power demand of 95 residential water heaters using a Kalman filtered neural network. The aggregation of water heaters was utilized in a pilot project in the city of Saint John, New Brunswick, which intended to provide more than 11 MW of ancillary services. In another work [44], the authors demonstrate the effectiveness of Dynamic Bayesian Networks to forecast the load demand of an aggregation of 1000 water heaters.

Load forecasting algorithms are typically classified according to their prediction horizons as very short-term load forecast (VSTLF), short-term load forecast (STLF), medium-term load forecast (MTLF), and long-term load forecast (LTLF) [41]. VSTLF and STLF are used for immediate decision-making processes, like balancing the electricity supply and energy trading. The cut-off horizon of short-term forecasts is two weeks [41]. STLF has received more research attention than the rest due to the deregulation of the utility grid and the lower need for LTLF. Furthest forecasting horizons (years) are used for capacity expansion, revenue analysis, and capital investment return studies [41].

Load forecasting methods are also classified according to the nature of the techniques they use: statistical or artificial intelligence (AI) techniques [45]. The validity of this classification has been argued; however, it is still extensively used in the literature [46]. Statistical techniques refer to traditional time series models, such as linear regression models [42], semiparametric additive models [41], autoregressive and moving average (ARMA) models [42], and exponential smoothing models [47]. AI techniques involve machine learning based models that do not need to have prior knowledge about the underlying relationship between the input and outputs variables [48]. This allows the creation of nonlinear fitting models with high accuracy [41]. Artificial neural networks (NNs) [49], fuzzy regression models [41], support vector machines [42], and gradient boosting machines [50] are well known AI techniques used in load forecasting. NNs have been used extensively in short-term load forecasts since the 1980s with many reports of successful applications [11]. NNs are data-driven techniques and can model complex nonlinear relationships between input and output vectors through a learning process [49].

The deployment of smart meters with the arrival of the smart grid has provided the industry with a vast amount of data. This new available data, together with more advanced computing and communications technologies, have facilitated the advent of hierarchical load forecasting (HLF). Traditional spatial load forecasting performs at the small area level or equipment, for example, at the distribution transformer. HLF, on the other hand, covers load forecasting at many levels, from household to utility level, and across various horizons, from minutes to years ahead [41].

Wind and solar generation forecasts have also been studied as part of the transition to a decentralized electric grid with higher renewable penetration [25]. The stochastic volatility of these distributed generation outputs can create balancing challenges on the grid. These challenges can be mitigated with the usage of demand response programs that also improve the system stability [32]. Accurate forecasts can help in dispatch optimization [51] and maximize renewable energy absorption [39], [52].

Load forecasting techniques usually produce their results as one forecasted value (single-step ahead forecasts) or a sequence of values (multi-step ahead) typically at equally spaced time steps. They are commonly referred as deterministic load forecasting algorithms. Over the past years, probabilistic load forecasting (PLF) has gained attention in the energy systems planning and operations [41]. PLF can be used mostly for stochastic unit commitment and power supply planning [41]. Instead of forecasting a single value, PLF provides the information in the form of quantiles [50], intervals [53], or density functions [41]. The main intervals used in forecasting are namely prediction intervals and confidence intervals. One way to evaluate the probabilistic outcomes is using Monte Carlo (MC) simulation [41], [54], [55]. This implies running many scenarios of deterministic load forecasts with random variation of the parameters according to their distribution functions. Each scenario has uncertainties associated with the initial conditions and the distribution of the parameters in the simulation. This method is often used as benchmark for comparison with other techniques in probabilistic load flow, where the exact load flow equation is known [56].

## 2.2 Aggregated DER Control

The progressive deregulation of the electric system has enabled the participation of distributed generation and controllable loads in energy markets. Many DERs can be aggregated into a single operating profile than can be managed by a VPP. A VPP serves as a dispatchable unit that responds to a designated system request, such as day-ahead dispatch or peak load reduction [57]. In this way, system operators can coordinate large numbers of DERs to optimize their consumption and decrease operation costs [58].

DLC enables operators to have direct control over the loads. Numerous DLC algorithms have been developed to determine the optimal control of aggregated residential loads. Most of them are based on linear programming [27], or dynamic programming [59], and target different load-shape goals, such as peak clipping [27], valley filling [60], load shifting [31] and flexible load shape [61]. These load shape objectives are usually combined to provide ancillary services to the energy system [18]. The control of the units is often accomplished via on/off signals [32], setpoints signals [62], or voltage controllers.

Load shifting is the focus of this thesis. It aims at rescheduling the demand from peak demand periods to low demand periods. Shifting the demand to a different time requires flexible loads that can be interrupted, such as water heaters, air conditioners, and space heating devices [32]. The control shifts what would have been conventionally consumed by these loads to a less critical time, usually to prior-to-peak period [63]. This tries to ensure that there are enough devices with sufficient energy stored during the curtailment time. Additionally, the customers would experience less discomfort due to the control actions compared to simply postponing the demand [10]. Still, the energy stored in the load might

be depleted after the curtailment period, when the control actions are no longer in effect. This could cause the reactivation of numerous appliances at the same time, producing a ‘rebound’ or ‘payback’ effect [43]. This payback effect could generate a large peak demand and it is difficult to manage if the on/off time of individual DERs is uncertain [38]. DER models can help manage the payback effect providing information that reduces the uncertainty in control activation [64], [65].

Load models have been used in the control of aggregated thermostatically controlled loads (TCLs) and electric vehicles [66], [67]. They provide an approximate physical model of the energy storage capacity that supports the prediction of their discharge and charge patterns [29]. The implementation of model-based controllers (MBCs) requires the identification of the model parameters. This can be done by measuring the state information or using estimation techniques (e.g., Extended Kalman Filter) [4].

DLC algorithms that depend on information measured at individual loads require complex sensing infrastructure. This raises privacy concerns regarding the data measured at end-user premises [10]. The increased amount of data sent over the data networks may introduce communication congestion and delay that may affect the efficacy of the algorithms [16]. Estimating the parameters and the states of individual load through models is an option. However, the uncertainties and stochastic end use affect the accuracy of the models and introduce errors in the estimated capacity of DERs.

### **2.3 Research Gaps**

Although many papers have contributed to the topic of aggregated DER demand forecast and control to provide ancillary services [24], [68], [69], few of them focus on the forecast

of aggregated DR capacity with probabilistic output. Most of the relevant studies focus on deterministic forecasts [22], [44], [45], [70]–[73] and require actual measurements to provide the estimated future load. Many of them use a single dispatch control strategy to estimate the peak reduction capabilities [38], [74]–[76] without analyzing the potential load shifting capacity of the resources [77], [78] or the effect on end-use comfort. The authors in [79], for example, focused on the performance of the proposed model in terms of accuracy but did not analyze its impact on user comfort. The results shown in [80] suggest that a good compromise between energy consumption and peak power can be obtained by properly selecting the setback temperature; however, no analysis of its implication on user comfort is presented. In the real-world implementation of residential TCLs for DR presented in [21] the authors evaluate customer comfort, but their control strategy does not include the user comfort as a performance parameter.

This thesis focuses on a probabilistic dispatch capacity forecast of aggregated DERs, with models that allow the simulation of individual loads and the estimation of their potential load shifting capacity during peak hours, while maintaining customer comfort.

### 3 Research Methodology

This chapter presents the design and methodology selected to comply with the objectives of the research. Section 3.1 presents the framework of this study, followed by the DER representation in section 3.2. Section 3.3 describes the strategy used to create the aggregation. Section 3.4 presents the control algorithms implemented to increase the dispatch capacity of the aggregation. Sections 3.5 and 3.6 present the forecasting algorithm and the experimental design respectively, followed by the evaluation method of end-user comfort in section 3.7. Finally, section 3.8 draws the conclusions of this chapter.

The aim of this study is to forecast the dispatch capacity of different aggregated DERs during peak demand periods. The estimation of the available aggregated DERs capacity is a complex challenge. Residential customers' loads have an intrinsic stochastic behavior which is difficult to model and forecast accurately. Their behavior is also affected by the control signals added in a DLC framework, which adds more complexity. Therefore, it is crucial for the forecasting method to understand and model the device's responsiveness and estimate the available aggregated capacity in the day-ahead market [57].

There are two main challenges regarding the forecast of aggregated DER dispatch capacity. The first challenge is how to model the responsiveness of the DERs to DLC signals, not only to modify their load demand, but also to analyze any discomfort caused to the customers. The second challenge is how to forecast the aggregated DERs dispatch capacity.

### **3.1 Framework**

It is necessary to consider the most representative characteristics of the environment in which the evaluated solutions are to be applied to have more realistic simulation results. SJE's LDN is currently the principal application scenario of the contributions of this work and therefore has served as the source of information to configure the proposed simulation scenario. Results of this study, however, are also applicable to other utilities seeking to improve their load factor by controlling aggregated residential loads.

#### **3.1.1 The Saint John Local Distribution Network (SJE's LDN)**

SJE intends to integrate DER into its distribution system to participate in DR programs with the objective of decreasing the peak in load consumption. Domestic electric water heaters, electric baseboard heaters, and electric thermal storage systems are among the embedded energy assets that are part of this program [26].

### **3.2 DER representation**

The DERs considered in this study will be modelled and studied using computer simulations. Every simulated individual load will be represented through digital implementation of mathematical models described in the scientific literature. This approach lets the simulation to keep track of the state of each DER, and it helps to analyze the effects in customer's comfort. The DERs that are part of this study are: domestic electric water heaters, electric baseboard heaters, and brick-core electric thermal storage systems.

### **3.2.1 DEWHs**

DEWHs can have more than one heating element. These devices are typically controlled by internal thermostats that operate based on pre-set temperature values. The thermostats implement a hysteresis band delimited by the lower and higher temperature values and serves to settle the ON and OFF states of the device. During the ON state only one element is turned on, so, in this study the DEWHs are represented by conventional single heating element units. The user interaction with the DEWH is simulated through a hot water usage model that is adapted to the average climate conditions and population distribution in New Brunswick. This way the simulation expresses the dependence of water withdrawal to weather conditions, number of household occupants, dissimilar hot water consumption habits, etc.

### **3.2.2 Electric baseboard heaters (EBHs)**

EBHs have two mayor types of operation: direct convection and hydronic. Convection heaters contain an electric heating element encased in metal pipes surrounded by aluminum fins to facilitate heat transfer [81]. In hydronic EBHs the heating element warms the liquid, water or oil, which in turn heats the air. The dynamics of EBH types are different: the hydronic type takes longer to heat up while in the convection type the heat dissipates quicker when the device is off. Convection type EBHs are more common in households and is the device considered in this thesis. EBHs are also the second most common (27%) heating source in Canadian homes, and the primary source in New Brunswick (66%) [82]. The equivalent thermal-electric analogy that uses Resistance-Capacitance (RC) modeling is the preferred choice to simulate the control of EBH [83]. This approach permits the

evaluation of baseboard heating systems using diverse types of thermostats and control strategies. This model can also be modified to denote distinctive characteristics and dimensions of buildings [80].

### **3.2.3 Electric Thermal Storage (ETS) systems**

There are several types of ETSs. ETS types vary depending on the storage medium: liquid or solid; device location: local in a room or central to heat the entire house; and the electric energy conversion method: using an electric heating element or a heat pump [84]–[87]. The brick-core ETS is the most common type of this device and is the one considered in this study.

### **3.3 Aggregation strategy**

The individual DERs will be aggregated with each aggregator consisting of only one type of DER. This allows analyzing each homogenous aggregator separately, as each DER will have different constraints in terms of user comfort and control signals. The conditions of the simulations (weather, hot water usage, setpoint temperatures, etc.) will be generated based on publicly available data and research studies. The model parameters will be randomly generated employing MC sampling. In this work, to generate MC scenarios we consider established distribution functions reported in the literature.

### **3.4 Control algorithms**

The objective of the control algorithms is to shift the load from peak hours to off peak hours while maintaining customers' comfort. To address the simulation of the responsiveness of the DERs to direct load control signals, this thesis focuses on model-

based controllers that take into consideration the approximate physical dynamics of a DER. This allows the generation of the baseline load, that is, the electricity that would have been consumed by the DER in the absence of DLC. The implementation of models also addresses the constraints of acquiring load data, since the actual data is private and may not be readily accessible. Once the baseline load model is obtained, a DLC program can be implemented to shift the load from peak hours to off-peak hours and estimate the response of the aggregator and its impacts on customer comfort.

The control algorithms evaluated in this thesis are the Direct Temperature Feedback Control (DTFC) [39] and the advanced DR setpoint control [21]. DTFC has been broadly implemented in practice for pilot projects [88]–[90] and has been used as a performance benchmark for other methods [90]. This algorithm is used to control DEWH and ETS in this study.

Several programs and pilot studies have been conducted involving the control of residential EBHs [33], [63], [81], [87], [90]–[93]. These studies focus on setpoint modulation strategies to achieve peak curtailment with minimum user discomfort. Overall, the participants experienced little discomfort in all the studies investigated. Strategies with ramps in the modulation signal have shown the lowest risk of users discomfort and great capacity for demand reduction [33], [94]. The advanced DR setpoint control algorithm [21], [91] is used in this study to shift the demand of EBHs from peak hours to off-peak hours.

### **3.5 Forecasting algorithm**

Multi-step ahead forecasts can be generated to form a probabilistic forecast when feeding multiple scenarios from a deterministic load forecasting model [41]. Each deterministic forecast will have the same probability as the equivalent input scenario. After several MC scenarios are generated and assigned equal probabilities, we can derive the important quantiles, such as the 10<sup>th</sup>, 50<sup>th</sup> and 90<sup>th</sup> percentiles [41], [95], [96]. In this study a short-term load forecaster with probabilistic output is used to forecast the aggregated DERs capacity. The target objective is to provide peak reduction capabilities that could help the system operator to increase the efficiency of the power grid.

### **3.6 Experimental design**

The simulations are designed to evaluate the veracity of the hypothesis of this study: Shifting the power demand of individual loads can increase the available aggregated dispatchable capacity without affecting customer comfort.

As a first step, the baseline load demand will be estimated from the aggregation of simulated DERs in the absence of DLC. The dispatchable capacity will then be calculated from simulation results by determining the difference between the baseline load demand and the load demand after applying a centralized control. The resulting forecasted capacity has additional uncertainties associated with the use of models that mimic the operation of real devices. The simulations yield dispatch capacity values that depend on the random distribution of the simulation conditions. An ensemble of multiple iterations will be implemented to estimate probable outcomes.

The available computing resources limit the number of iterations  $N$  selected for the MC experiments. The mean value of a population is estimated from a sample obtained from the  $N$  iterations in an MC experiment. The confidence interval  $(L, U)_{CL}$  for the sample mean  $\bar{x}$  for a confidence level is [97]:

$$(L, U)_{CL} = \bar{x} \pm z_c \frac{S_x}{\sqrt{N}} \quad (3.1)$$

where  $S_x$  is the sample standard deviation,  $z_c$  is the z-score associated to the confidence level. The maximum percentage error of the sample mean is computed as

$$E = 100 \times z_c \frac{S_x}{\bar{x}\sqrt{N}} \quad (3.2)$$

Equations (3.1) and (3.2) serve to compute the maximum errors in the estimation of the means of the dispatched capacity in the MC experiments for a confidence level of 95% ( $z_c = 1.96$ ). The errors can be further reduced increasing the number of iterations. Each iteration is assigned the same probability.

### 3.7 End-user comfort evaluation

End-user comfort is evaluated according to the specific usage of the device. For instance, in DEWHs, the water temperature should remain above a certain threshold to provide sufficient hot water to the customer. End-user comfort can be maintained if the water temperature is above the minimum threshold [90]. However, periods of high water demand can lower the temperature below the minimum value [98]. The duration below this minimum threshold should not increase significantly when external control actions are applied.

The estimation of thermal comfort of the customers using space heating devices is a complex process. Thermal comfort is defined by ASHRAE [99] as: “the condition of mind in which satisfaction is expressed with the thermal environment”. In other words, thermal comfort depends on both the surrounding environment and the person. There are different thermal comfort models that have been studied in the literature. The predicted mean vote (PMV) [94] index includes six parameters that influence the thermal comfort: air temperature, mean radiant temperature, relative humidity, air velocity, metabolic rate, and clothing insulation. This approach is commonly referred to as the rational approach. Other thermal comfort models include the standard effective temperature [100] and the human thermal comfort models proposed in [101]. Due to the complexity of these models, in this thesis the end-user comfort with EBHs is evaluated through the deviation of the room temperature from the temperature setpoint, considering acceptable a difference of less than 1°C [102]–[105]. This reduces the complexity of the thermal-comfort estimation to only account for the room temperature, neglecting other parameters that are difficult to measure. On the other hand, the end-user comfort with ETS can be maintained if the core temperature doesn't violate the lower deadband of the comfort level. The ETS functions as a thermal storage, whenever more heat is needed, its built-in fan will blow hot air through the core and into the room. The core's temperature must remain high enough to supply the heat to the room as needed by the customer.

### **3.8 Chapter Conclusions**

The research methodology selected aims to form scenarios of homogeneous DERs aggregations based on model representations and computer simulations. The proposed

approach finds the baseline load demand first and then evaluates the effect of control algorithms on the dispatch capacity. DFTC and Advanced DR setpoint control algorithms will be evaluated through Monte Carlo experiments.

User comfort will be evaluated according to the specific usage of each type of DER and is quantified through deviation of observed temperature from thermostats setpoints. The percentage error is used to validate the experimental results.

## 4 Aggregate DER Demand Forecast

This chapter presents the modeling of individual and aggregated DERs. Section 4.1 introduces the modeling of DEWHs. Section 4.2 presents the modeling of EBHs. Section 4.3 describes the modeling of ETSs. Section 4.4 draws the conclusions of this chapter.

### 4.1 Domestic Electric Water Heaters (DEWHs)

This section includes the description of the model of DEWH, from the individual device to the aggregation level.

#### 4.1.1 Modelling of DEWHs

The modelling of DEWHs has been researched widely [59], [60], [98], [106], [107]. A single element water heater is presented in [106]. This model assumes there is a single layer of water with uniform temperature. Therefore, the rate of change of the water temperature inside a DEWH is affected by heat losses, incoming power, and inlet water temperature:

$$\dot{T}(t) = \frac{P_e(t)}{C_p \rho V} + \left( \frac{G}{C_p \rho V} \right) (T_a - T(t)) + \left( \frac{q(t)}{\rho V} \right) (T_{in} - T(t)) \quad (4.1)$$

Where  $P_e(t)$  is the power of the unit (W),  $G$  is the surface thermal conductance (W/°C),  $T_a$  is the ambient temperature outside the DEWH (°C),  $T(t)$  is the water temperature inside the DEWH (°C),  $T_{in}$  is the temperature of the inlet water (°C),  $q(t)$  is the water mass flow rate (kg/s),  $C_p$  is the specific heat capacity of water (J/kg°C),  $\rho$  is the water density (kg/m<sup>3</sup>), and  $V$  is the tank's volume (m<sup>3</sup>). The thermostat's on/off states are governed by its hysteresis control as follows:

$$P_e(t) = \begin{cases} P_{rated}, & T(t) \leq T_{min} \\ 0, & T(t) \geq T_{max} \\ P_e(t^-), & otherwise \end{cases} \quad (4.2)$$

where  $P_{rated}$  is the rated power of the unit,  $P_e(t^-)$  is the previous value of  $P_e(t)$ , and  $T_{min}$  and  $T_{max}$  represent the lower and higher limits of the hysteresis temperature band, respectively. The temperature of the water decays and increases between these limits during no water demand operation, as shown in Figure 4.1.

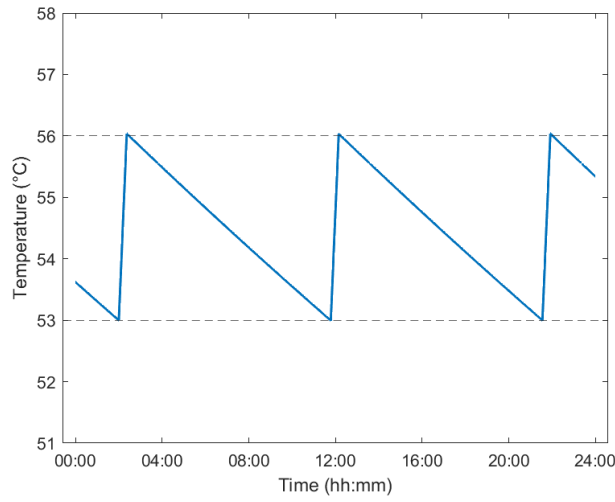


Figure 4.1: Temperature of water in the tank with no water usage.

The aggregate DEWH model was developed using the individual model described in equation (4.1). The parameters of the tanks were randomized uniformly according to Table 4.1. The randomization increases the diversity of the aggregation, as occurs in a real population, and decreases the on/off synchronization of DEWHs [31], [38], [108]. The model considers correlation between tank's volume and its rated power; for instance, a water heater with a large tank will have a high-powered heating element.

Table 4.1: Parameters of DEWHs.

Simulation parameter	Meaning	Value
$T_a$	Ambient temperature	15-25 °C
$T_{in}$	Inlet water temperature	5-10 °C
$T_{set}$	Thermostat setpoint	50-60 °C
$T_{hb}$	Thermostat hysteresis band	5 °C
V	Tank volume	200/227/300 Liters
$P_{rated}$	Rated power	3/4.5/4.8 kW
G	surface thermal conductance	3.5 W/°C

#### 4.1.2 Hot Water Usage Model

The use of a hot water demand model allows the simulation of hot water consumption for each DEWH in the aggregation. References [109], [110] provide a thorough study of the hot water demand profiles used in this study. They provide general models that can be applied to approximate the amount of hot water consumption in a household. According to [109], the fraction of water used for bathing, showers and faucet is determined as follows:

$$F_{mix} = 1 - [(T_{set} - T_{mix}) / (T_{set} - T_{mains})] \quad (4.3)$$

where  $F_{mix}$  is the fraction of occupancy uses that are hot based on water inlet temperatures,  $T_{set}$  is the hot water supply temperature (°C),  $T_{mix}$  is the targeted water temperature at point of use, generally assumed to be 40.6°C (105°F) [109], and  $T_{mains}$  is the inlet mains water temperature (°C). Equation (4.4) describes the procedure to estimate  $T_{mains}$ , based on the study presented in [110].

$$T_{mains} = (T_{amb,avg} + offset) + ratio \times \left( \frac{\Delta T_{amb,max}}{2} \right) \dots \quad (4.4)$$

$$\dots \times \sin(0.986 \times (day\# - 15 - lag) - 90)$$

where  $T_{mains}$  is the supply temperature to DEWH (°C),  $T_{amb,avg}$  is the annual average ambient air temperature (°C),  $offset$  is 3.3°C [6°F],  $\Delta T_{amb,max}$  is the maximum difference between monthly average ambient temperatures (°C),  $day\#$  is the Julian day of the year (1-365). Reference [110] indicates that  $day\#$  should be found using equation (4.5) for models using average monthly mains temperature.

$$day\# = 30 \times month\# - 15 \quad (4.5)$$

where  $month\#$  is the month of the year (1 to 12). The  $ratio$  and  $lag$  factors can be determined using equations (4.6) and (4.7) respectively. These factors were determined by fitting the available data in [110], and are consistent with water pipes being buried deeper in colder climates.

$$ratio = 0.4 + 0.01 \times (T_{amb,avg} - 44) \quad (4.6)$$

$$lag = 35 - (T_{amb,avg} - 44) \quad (4.7)$$

Figure 4.2 shows the values of monthly mains temperature profile and  $F_{mix}$  for Saint John, New Brunswick, using typical meteorological year (TMY) data taken from [111]. In this case,  $F_{mix}$  averages 0.7365, 0.0831% higher than the 0.68 value found in [109] where most of the inlet water temperatures were measured in warmer sites.

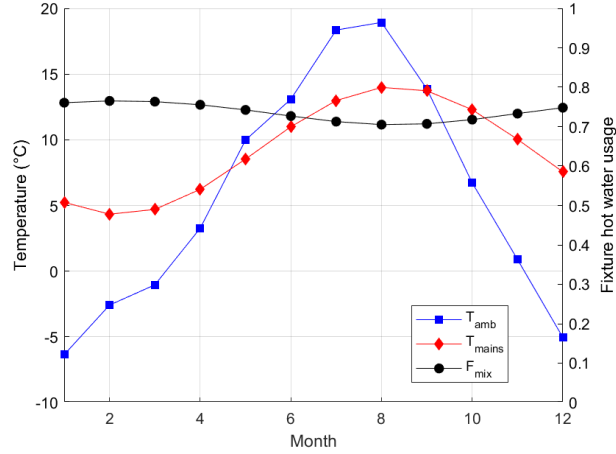


Figure 4.2: Monthly mains water temperatures and  $F_{mix}$  values using TMY data for Saint John, NB.

The value of  $F_{mix}$  is used to calculate the total amount of hot water used in a household per day [109], as follows:

$$HW_{lpd} = 83.27 \times (Occ \times F_{mix}) + c \quad (4.8)$$

where  $HW_{lpd}$  is the total hot water used in liters per day,  $Occ$  is the number of occupants in the house, and  $c$  is a random error that takes values from 0 to 38 liters with a uniform distribution, and accounts for usage of standard clothes washer and dishwasher [109]. Figure 4.3 (Left) shows the percentage of the population corresponding to the number of occupants in a household and the boxplot of  $HW_{lpd}$  values. The number of occupants in the households were estimated based on Saint John's 2016 census data available at [112].

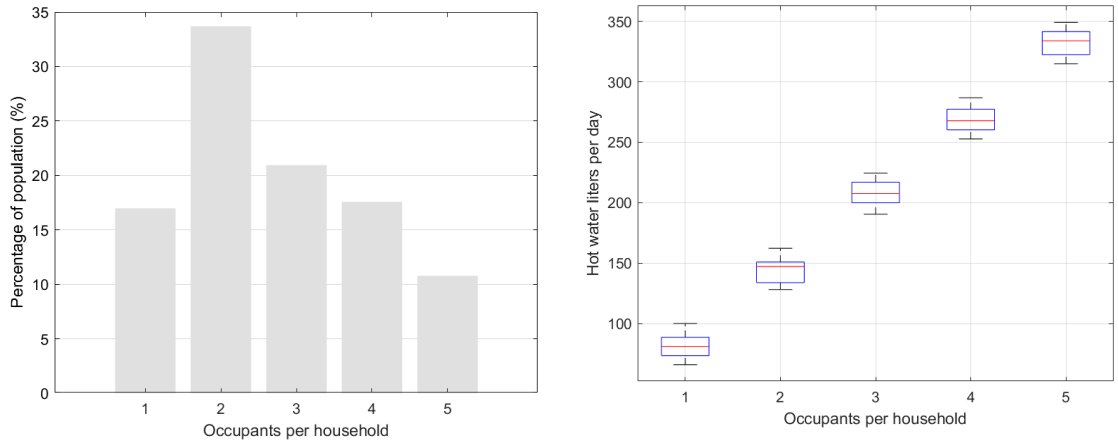


Figure 4.3: Left: Distribution of population vs. occupants. Right: Box plot of liters of hot water usage per day vs. number of occupants.

The total hot water usage per household is then divided into smaller volumes based on predefined probability distributions (Figure 4.4). The model presented in this study describes the daily hot water usage profile for individual DEWH according to three different user patterns: morning, evening, and dispersed [113], [114]. Each pattern assigns a hot water draw event probability for each hour of the day. These patterns are randomly assigned to each DEWH to guarantee variety of user behaviors.

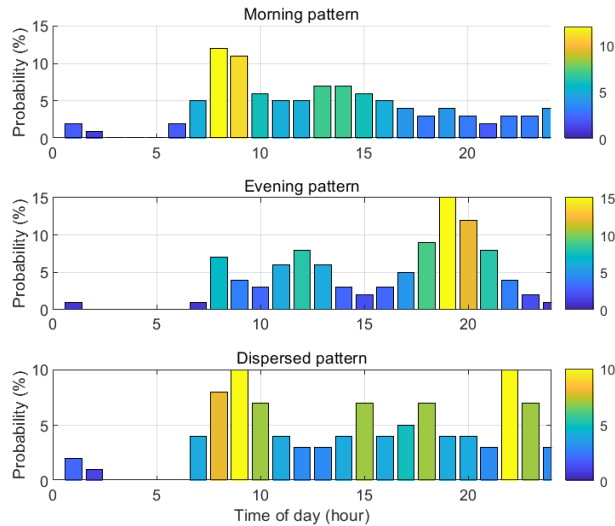


Figure 4.4: Hot water draw event probability distributions.

Figure 4.5 shows the average daily profile of 2000 simulated hot water withdrawal profiles. This average profile is characterized by high usage in the morning and evening, and low water usage at night. The daily water consumption related to this average profile is 196 liters, which is in accordance with the values found in [39], [109], [115], [116].

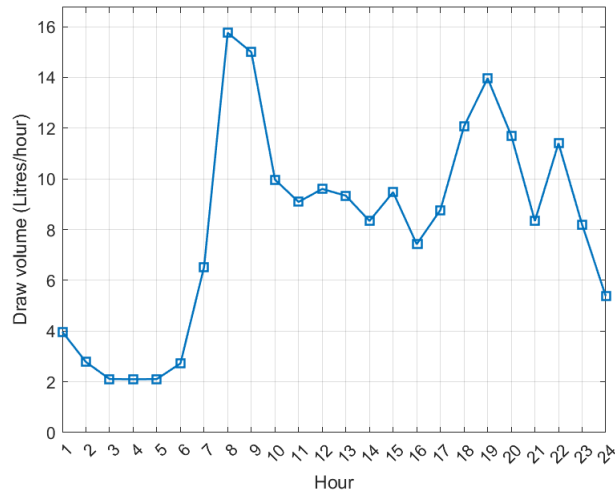


Figure 4.5: Average daily hot water consumption profile.

### 4.1.3 Diversified demand of DEWHs

The individual daily electricity demand of DEWHs is simulated with the models described previously. The aggregated electricity profiles give the diversified daily demand of a population of water heaters. Still, the initial states of the devices need to be determined to run the simulation. In this thesis, the initial water temperature is randomized uniformly within the deadband. Initial on/off states are randomized uniformly with 12% of DEWHs being on. This percentage was found when running the simulation for one day and getting the number of devices ON at 24:00 hours, where the aggregation is stable and not affected by the response to, probably unrealistic, initial conditions. This intends to avoid the initial high demand produced when initializing 50% of the water heaters ON [31], [117], which

is higher than the usual peak of the aggregation. Figure 4.6 illustrates the simulated aggregated water demand and the corresponding aggregate power demand of a population of 2000 DEWHs. This power demand will be referred to as the autonomous demand of the population [39].

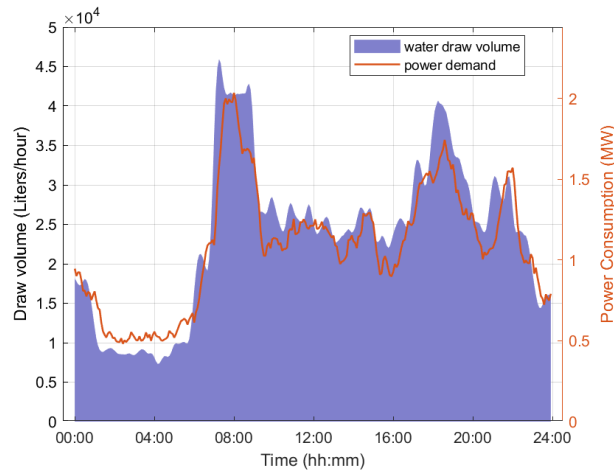


Figure 4.6: Simulated aggregate water draw for 2000 DEWHs over 24 hours and the corresponding total power demand of the population (autonomous demand).

## 4.2 Electric Baseboard Heaters (EBHs)

The next sections present the model used to represent the EBH and the aggregation approach that mimics the diversified demand produced by this type of device.

### 4.2.1 Modelling of EBH

The equivalent Resistance-Capacitance network is one of the most common approaches to model the thermal dynamics in a building [80], [87], [92]. The RC circuit analogy represents an equation where resistances act as the areas of thermal transfer between zones, and capacitances serve as the thermal masses within every zone [66], [87]. Figure 4.7 shows the equivalent RC used for a room heated by a single EBH. This system is a

simplified version of the RC circuit found in [87]. The heat losses through interior walls (walls connected to adjacent rooms) are neglected. Equation (4.9) is used to represent the energy balance in the room.

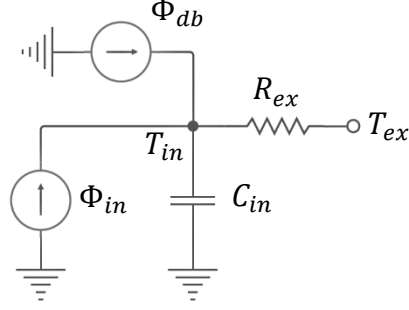


Figure 4.7: RC network for a room with an EBH.

$$C_{in}\dot{T}_{in} = \frac{T_{ex} - T_{in}}{R_{ex}} + \Phi_{in} + \Phi_{db} \quad (4.9)$$

where,  $C_{in}$  is the thermal capacitance of the room (J/K),  $T_{in}$  is the internal air temperature of the room (K),  $T_{ex}$  is the exterior air temperature (K),  $R_{ex}$  is the equivalent total thermal resistance of the room (K/J/s),  $\Phi_{in}$  is the heat flow produced by the EBH (J/s), and  $\Phi_{db}$  (J/s) is the total gains from thermal disturbance sources such as sunlight irradiance and other sources of heat. The value of  $\Phi_{db}$  is not measurable for most real applications [87]. Although it could be estimated [118], it is neglected in this study to avoid introducing uncertain variables. The heating power of the EBH is governed by the hysteresis control as described in equation (4.2). The efficiency of the EBH is considered as 100% [87]. The values of thermal resistance and thermal capacitance of each room are calculated according to [119]:

$$R_{ex} = \frac{1}{\sum A_i U_i}, \quad C_{in} = m_a c_p \quad (4.10)$$

where  $A_i$  ( $m^2$ ) is the surface area of the region exposed to outdoor air temperature (external walls, windows, etc.),  $U_i$  is the U-value (thermal transmittance) of said region ( $W/m^2K$ ),  $m_a$  is the air mass inside the room (kg), and  $c_p$  is the specific heat capacity of air ( $J/kgK$ ). Figure 4.8 shows the air temperature in a simulated room with a single EBH with a setpoint of  $20.76^\circ C$  and a hysteresis band of  $1^\circ C$ .

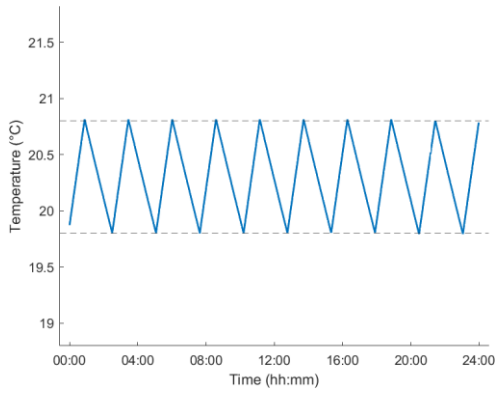


Figure 4.8: Room temperature with one EBH and a constant outdoor temperature of  $0^\circ C$ .

#### 4.2.2 Diversified demand of EBHs

The aggregate EBH model was developed using the individual model described in equation (4.9). The parameters of the rooms were generated with uniform distribution within the ranges provided in Table 4.2.

Table 4.2: Parameters of EBHs and rooms.

<b>Parameter</b>	<b>Value</b>
Thermostat setpoint	18 - 24 °C
Thermostat hysteresis band	1 °C
<b>Room parameters</b>	
Length	3 - 4.6 m.
Width	3 - 4.6 m.
Height	2.44 - 3 m.
Window area	0.84 - 1.64 sq. m.
Door area	1.3 - 1.67 sq. m.
<b>Thermal properties</b>	
<b>Region</b>	<b>U-value (W/m<sup>2</sup>K)</b>
Door	1.32 - 1.8
Floor	0.3311 - 1.321
Roof	0.5 - 1.321
Wall	0.641 - 1.321
Window	1.2 - 1.8

The simulation assumes that each room has at least one wall exposed to the exterior air temperature, and a maximum of two exposed walls. Every room has one window.

There are various methods to find the proper sizing of heating systems [19], [80], [87]. These procedures range from methods that require a detailed knowledge of the building and occupancy [80], to empirical methods that consider only the room surface area [19]. Regardless of the method used, the size of the heating load must always maintain the comfort quality of the users. The heating power of the EBH in this study is estimated according to [119]:

$$P_{rated} = \frac{T_{set} - T_{design}}{R_{ex}} \quad (4.11)$$

where  $T_{set}$  is the thermostat setpoint (K),  $T_{design}$  is the winter design temperature according to the building code of the region (K), and  $R_{ex}$  is the thermal resistance of the room (K/W).  $T_{design}$  sets the value above which the outdoor temperature stays for 99% of the hours in the year [120]. This means that the outdoor air temperature is going to be colder than  $T_{design}$  for only 1% of the hours in a year. Figure 4.9 shows the distribution of the heating power of the EBHs based on equation (4.11) and the factors in Table 4.2.

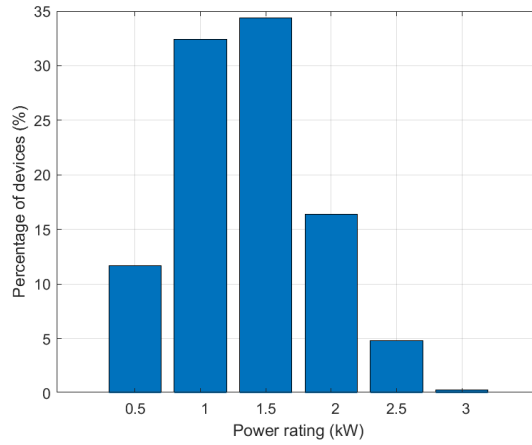


Figure 4.9: Power rating distribution of EBHs.

The setpoint schedule of the customers is created based on the work presented in [63], which demonstrates how in a pilot project conducted in Quebec, the customers applied a setback and pick-up schedules in their programmable thermostats to save power. The authors of [63] show that most of the occupants apply a single night setback schedule. It also reveals that the morning pick-up hour is concentrated around 6:30 a.m. Figure 4.10 displays the magnitude of the thermostat setbacks. The occupants usually decrease the

thermostat setpoint 2 or 3°C below the comfort temperature during the night and set the pick-up hour thirty minutes before they wake up.

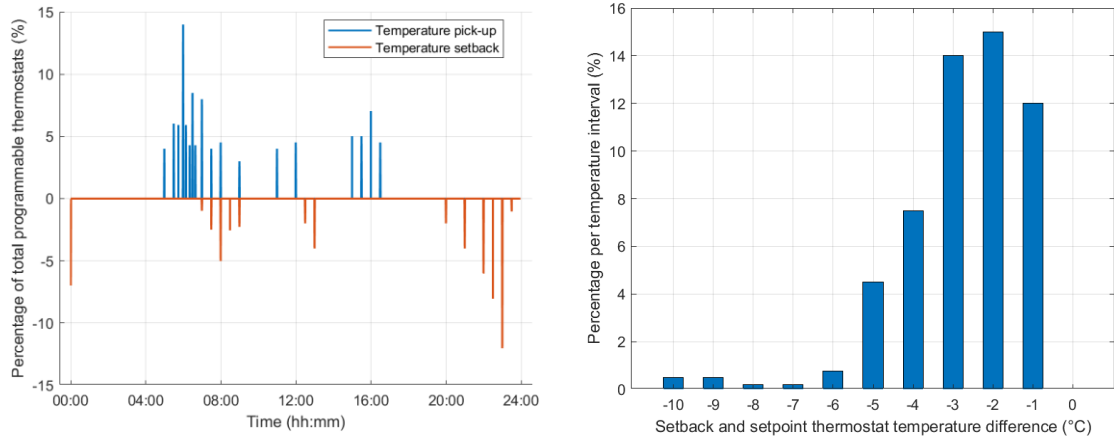


Figure 4.10: Left: Distribution of pick-up and setback hours. Right: Distribution of temperature differences between setback and setpoint.

The room temperature is initialized as the setpoint temperature. The initial on/off states are also randomized uniformly with 50% of EBHs being on. Figure 4.11 shows the autonomous demand of a population of 200 EBHs for a particular day.

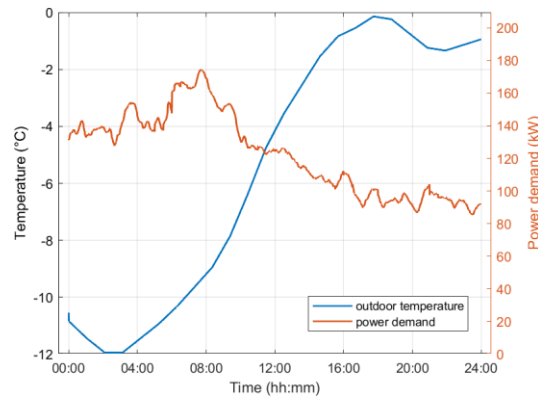


Figure 4.11: Outdoor temperature and corresponding autonomous demand of 200 EBHs.

### 4.3 Electric Thermal Storage (ETS).

The following sections present the model of brick-core ETS systems considered in this study and the aggregation methods implemented.

#### 4.3.1 Modelling of ETSs.

ETS stores thermal energy in high-density bricks. The heat is generated by electric heating elements placed between the bricks [85], usually during low electricity price periods or off-peak hours. A thermostat-controlled fan then blows air through air channels in the bricks to discharge the stored heat into the room (Figure 4.12).

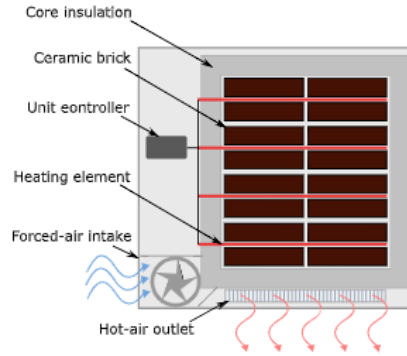


Figure 4.12: Electric Thermal Storage [87].

The thermal dynamics of a zone with an ETS depend on the heat transfer between the heating elements of the ETS and the bricks, the heat transfer between the bricks and the supplying air, and the heat transfer between the air in the zone and the external ambient temperature, as described in equations (4.12) - (4.14).

$$m_b C_{pb} \frac{dT_b}{dt} = U_b A_b (T_s - T_b) + r_e q_e \quad (4.12)$$

$$m_s C_p \frac{dT_s}{dt} = U_b A_b (T_b - T_s) + r_s \dot{a}_s C_p (T_z - T_s) \quad (4.13)$$

$$m_z C_p \frac{dT_z}{dt} = \dot{a}_v C_p (T_{ex} - T_z) + r_s \dot{a}_s C_p (T_s - T_z) + \sum_{i=1}^N U_i A_i (T_{ex} - T_z) \quad (4.14)$$

where  $m_b$  is the mass of bricks (kg);  $C_{bp}$  is the specific heat of bricks (J/kg/°C);  $T_b$  is the temperature of bricks (°C);  $U_b$  is the heat transfer coefficient of bricks (W/m<sup>2</sup>/°C);  $A_b$  is the surface area of the bricks (m<sup>2</sup>);  $T_s$  is the temperature of the supplying air (°C);  $r_e$  is the on/off state of the heating element;  $q_e$  is the rated power of the heating element (W).  $\dot{a}_s$  is the flow rate of the air from the outlet to the zone (kg/s);  $C_p$  is the specific heat of air (J/kg/°C);  $r_s$  is the open/close state of the damper;  $T_z$  is the zone temperature (°C);  $m_z$  is the air mass in the zone (kg);  $\dot{a}_v$  is the air flow due to ventilation (kg/s);  $T_{ex}$  is the external air temperature (°C);  $N$  is the number of building elements (walls, windows, doors...) exposed to external air temperature;  $U_i$  is the heat transfer coefficient of the  $i_{th}$  element (W/m<sup>2</sup>/°C) and  $A_i$  is the surface area of the element (m<sup>2</sup>).

Figure 4.13 shows the diagram of the ETS model. This model ignores the heat transfers inside the unit, simplifying the model to account only for the heat losses through the building envelop (room heat losses) and resulting in equation (4.15).

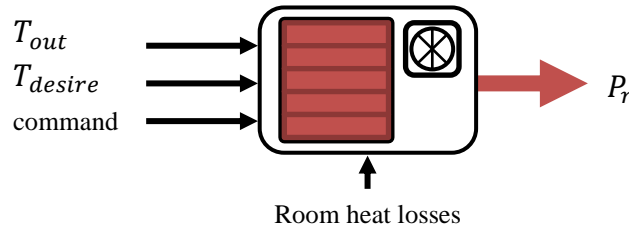


Figure 4.13: Simplified model of ETS.

$$\eta_e \int_0^{t_{on}} q_e dt = \int_0^{t_{off}} h_t dt \quad (4.15)$$

where  $\eta_e$  is the efficiency of the heating elements;  $q_e$  is the rated power of the heating element (W);  $h_t$  are the total room heat losses (W), which primarily depends on room size, insulation level and weather;  $t_{on}$  and  $t_{off}$  are the periods of ETS under ON and OFF operation, respectively. The heat leakages from the ETS core to the zone environment are not considered losses in the traditional sense since they still contribute to heat the zone [84]. The output heat flow from the ETS is determined according to the outdoor temperature, the setpoint temperature, the zone net heat losses and the ETS nominal rated power. The external control signal represents the on/off command coming from the upper level (e.g., DLC controller). Figure 4.14 shows the temperature of the bricks of a single ETS with a constant outdoor temperature of 0°C and a desired room temperature of 23°C. The on/off control of the ETS can be manual or automatic. In manual control, the owner sets the desired level of charge during the heating period. The automatic control regulates the core charge level according to the outdoor temperature. An outdoor sensor reads the value of the temperature and sends it to the control unit that actuates on the heater to adjust the core temperature appropriately [121].

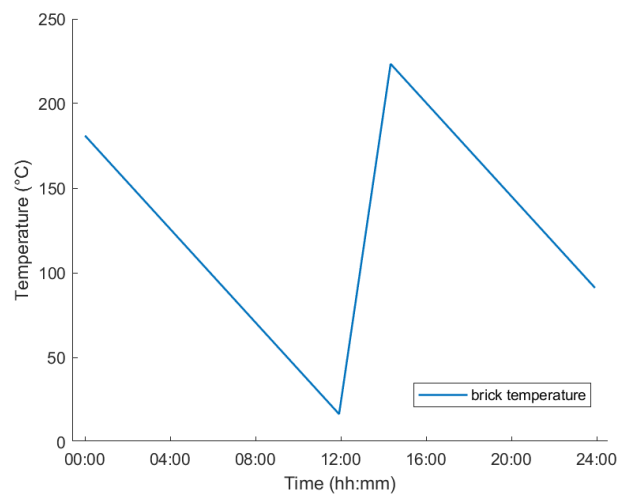


Figure 4.14: Bricks' temperature in an ETS with a constant outdoor temperature of 0°C.

### 4.3.2 Diversified demand of ETSs

The aggregate ETS population was developed using the individual model represented in Figure 4.13. The size of each ETS is selected following the guidelines of the manufacturer [122] considering the thermal requirements of the room. Typical brick-core ETS vary in size from 1.32 to 10.8 kW [85]. The size of the room is set following the dimensions and thermal properties described in Table 4.2, with a uniform distribution. The initial brick temperature is randomized uniformly within the deadband. The initial ON/OFF states are also randomized uniformly with 50% of ETSs being on. Figure 4.15 shows the outdoor temperature of a particular cold day and the corresponding autonomous demand of a population of 50 ETSs.

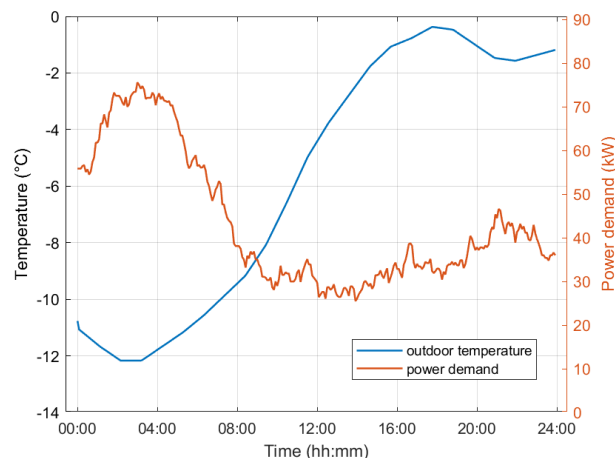


Figure 4.15: Outdoor temperature and corresponding autonomous demand of 50 ETSs.

## 4.4 Chapter Conclusions

This chapter has provided the individual and aggregated models of DEWHs, EBHs and ETSs implemented in the simulations. Device model and usage parameters were selected according to the SJE scenario, the same applies to meteorological information.

The demand for each type of device is diversified through parameters randomization.

The focus will now be shifted in the next chapter to the development and simulation of the control strategies to forecast the aggregators' dispatch capacity.

## **5 Aggregate DER Control and Dispatch Capacity Forecast**

This chapter describes the control algorithms implemented to forecast the dispatch capacity of aggregated DERs. Section 5.1 shows a detailed description of Direct Temperature Feedback Control algorithm that is used to control aggregated DEWHs. This algorithm is also employed to control aggregated ETSs in this study, due to their high thermal storage capacity. Section 5.2 explains the control algorithm used in aggregated EBHs. Sections 5.3 to 5.5 present the dispatch capacity forecast of aggregations of DEWHs, EBHs and ETSs respectively, including the analysis of the impact in customers' comfort. Section 5.6 presents the implemented planning tool that can be used to forecast the dispatch capacity based on user inputs. Section 5.7 draws the conclusions of this chapter.

### **5.1 Direct Temperature Feedback Control**

Although the description of the algorithm is intended for water heaters, DTFC can be easily coupled with ETSs. Instead of measuring water temperature, the control would work with bricks temperature. DTFC requires sensor data for the water temperature, the temperature deadband limits, and the rated power of each unit. The on/off state of each water heater depends on the reference power (desired aggregate demand for the current time step), their current water temperature, and their rated power. This algorithm consists of two parts: (i) selection of subset of DEWHs that is available for external control, and (ii) the ranking of this subset to identify the DEWHs that will be controlled. The controller divides the water heaters into subsets based on their temperature and on/off state (Table 5.1).

Table 5.1: DEWHs subsets.

$N$	Set of all water heaters
$N_{on,t}$	Set of all water heaters that are currently on
$N_{off,t}$	Set of all water heaters that are currently off
$N_{hot,t}$	Set of all water heaters with $T \geq T_{max}$
$N_{cold,t}$	Set of all water heaters with $T \leq T_{min}$
$N_{db,t}$	$N - (N_{hot,t} \cup N_{cold,t})$ . Set of water heaters within the deadband

The following subpopulations are then derived:

$$N_{th,on,t} = N_{off,t} \cap N_{cold,t} \quad (5.1)$$

$$N_{th,off,t} = N_{on,t} \cap N_{hot,t} \quad (5.2)$$

where  $N_{th,on,t}$  and  $N_{th,off,t}$  represent the groups of water heaters that are violating the deadband temperature limits and will be switched on and off by their internal thermostatic controllers. The sets of DEWHs that are available to the controller are defined as:

$$N_{av,off,t} = N_{on,t} \cap N_{db,t} \quad (5.3)$$

$$N_{av,on,t} = N_{off,t} \cap N_{hot,t} \quad (5.4)$$

The next step in the algorithm decides which devices should be turned on or off. The next description outlines this procedure:

1. The difference between the reference power ( $P_{ref,t}$ ) and the actual aggregate power of the population ( $P_{agg,t}$ ) is computed at each time step:

$$\Delta P_t = P_{ref,t} - P_{agg,t} \quad (5.5)$$

2. Considering the thermostat switching actions of (5.1) and (5.2), the effective difference in power that needs to be achieved by additional switching actions is equal to:

$$\Delta P_{ef,t} = \Delta P_t + P_{th,off,t} - P_{th,on,t} \quad (5.6)$$

where  $P_{th,off,t}$  is the total power of DEWHs that belong to the set  $N_{th,off,t}$  and  $P_{th,on,t}$  is the total power of DEWHs in  $N_{th,on,t}$ . If  $\Delta P_{ef,t} < 0$  additional switching off action is required. Conversely, if  $\Delta P_{ef,t} > 0$ , switching on action is desired.

3. The algorithm determines the final list of water heaters that will be switched as follows:

- If  $\Delta P_{ef,t} < 0$ , the DEWHs in the set  $N_{av,off,t}$  are ranked in descending order according to  $(T_{i,t} - T_{min,i})$ , such that the hotter the DEWH is, the higher its switching off priority. The final list of water heaters that will receive a switch off signal  $N_{sw,off,t}$  is determined by selecting the number  $N_{d,t}$  of devices from the ordered list that minimizes:

$$\left| \Delta P_{ef,t} + \sum_{i=0}^{N_{d,t}} P_{r,i} \right| \quad (5.7)$$

where  $P_{r,i}$  is the rated power of the  $i^{th}$  water heater in the list.

- If  $\Delta P_{ef,t} > 0$ , the DEWHs in the set  $N_{av,on,t}$  are ranked in ascending order according to  $(T_{max,i} - T_{i,t})$ , such that the colder a DEWH is, the higher is switching on priority. The set of water heaters that will receive a switch on signal  $N_{sw,on,t}$ , is determined by selecting the number  $N_{d,t}$  of devices from the ordered list that minimizes:

$$\left| \Delta P_{ef,t} - \sum_{i=0}^{N_{d,t}} P_{r,i} \right| \quad (5.8)$$

4. The controller then sends the switching signal  $u_{i,t}$  to each DEWH according to:

$$u_{i,t} = \begin{cases} 1, & \text{if } i \in N_{sw,on,t} \cup N_{th,on,t} \\ 0, & \text{if } i \in N_{sw,off,t} \cup N_{th,off,t} \\ u_{i,t-1}, & \text{otherwise} \end{cases} \quad (5.9)$$

## 5.2 Advanced DR setpoint control

The control strategy used is a modified version of the advanced DR strategy in [21], [91]. This strategy was selected because it offered great potential for peak reduction with little customer discomfort reported. Figure 5.1 shows the set of rules implemented to produce the control schedule. These rules are based on the work in [21], with modifications to fit the circumstances of this study: the decrease interval was extended to finish at the end of the peak period, instead of at the middle of the peak hours to increase the dispatch capacity; a random delay between 0 to 1.5 hours was added to the pick-up ramp at the end of the peak period to reduce the payback effect [63]. Equations (5.10) to (5.13) complement the rules depicted in Figure 5.1.

$$t_{pa} = t_{ps} + 0.5 \quad (5.10)$$

$$t_{pb} = t_{pe} - 0.5 \quad (5.11)$$

$$t_{pc} = t_{pa} - 2 \quad (5.12)$$

$$t_{pd} = t_{ps} - 0.75 \quad (5.13)$$

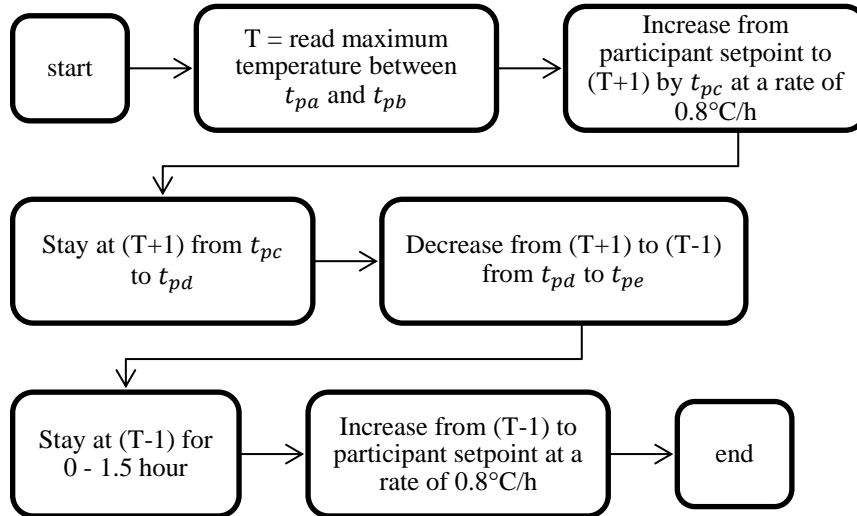


Figure 5.1: Rules used to create the setpoint control schedule.

where  $t_{ps}$  is the start of the peak period (hours) and  $t_{pe}$  is the end of the peak period (hours).

Figure 5.2 shows the DR schedule applied to a constant and non-constant customer-defined schedules assuming a peak period from 7 a.m. to 9 a.m.

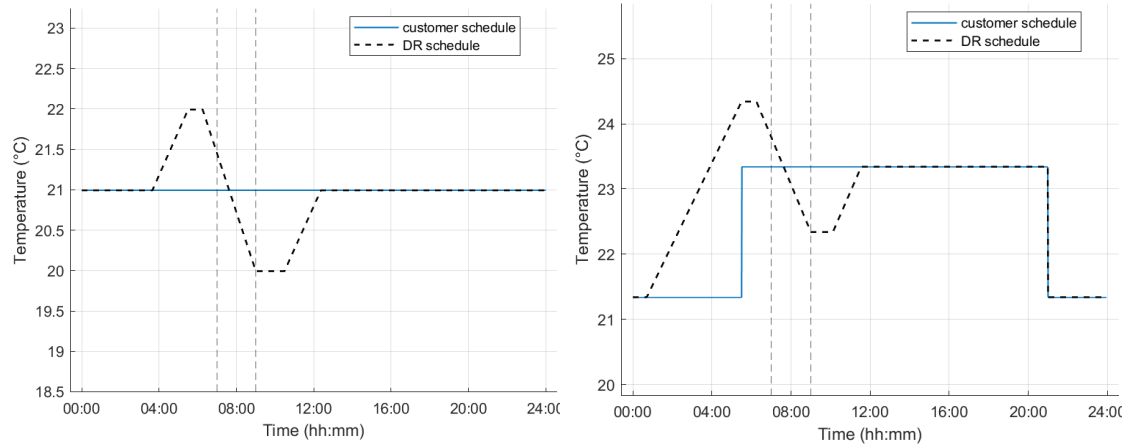


Figure 5.2: Left: DR schedule designed to a constant customer schedule. Right: DR adapted to a dynamic customer schedule.

### 5.3 Dispatch capacity forecast of DEWHs

The storage capacity of DEWHs in the form of thermal energy allows them to be pre-heated during times of low hot water consumption. The pre-heat phase is intended to increase the water temperature of a DEWH to the maximum threshold temperature by the start of the peak. This can raise the time it takes for the water heater to reactivate, lower the chances of running out of hot water during the peak period, and decrease the payback effect. Figure 5.3 illustrates the effects of applying a pre-heat period compared to a control without pre-heat. The dispatch capacity is larger with pre-heat, and the amplitude of the payback is smaller. The water temperature of DEWHs will be close to the minimum threshold if the external controller increases their off time in periods of high-water usage. Therefore, most of the water heaters will turn on when the external control is released. This large payback effect needs to be mitigated to avoid introducing a new peak in the load.

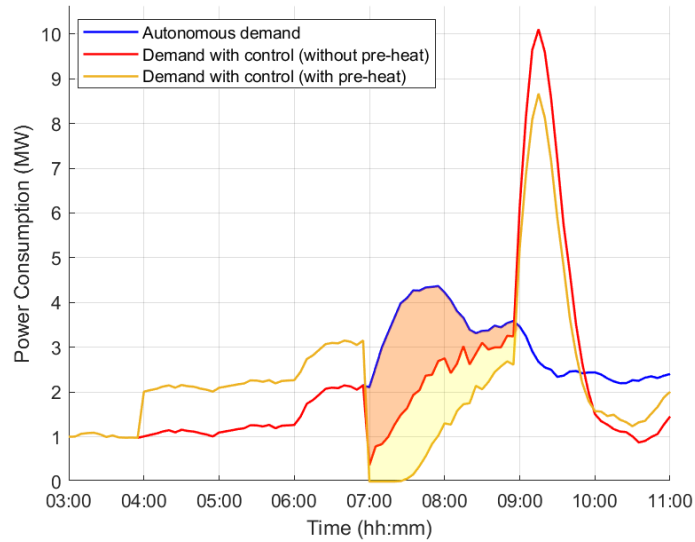


Figure 5.3: Comparison between the aggregate power demand of 4000 DEWHs with and without pre-heat period.

The DLC algorithm was implemented to follow a reference power with the objectives of pre-heating the water heaters, reduce the power during the peak period and limit the payback effect. The reference power during the pre-heat period is created with a value higher than the autonomous demand. The controller will turn on additional water heaters to match the reference power. This will increase the ON time of DEWHs, thus, rising their water temperature steadily. The same process is used to mitigate the payback effect. The reference power during the peak period is set to 0 Watts. Figure 5.4 shows a diagram of the DLC strategy. The autonomous demand is represented by a line for simplification. The amount of power above the autonomous demand during the pre-heat and recovery periods depend on the available time to control, the size of the aggregation, and the maximum power that the VPP is willing to commit without incurring in excessive costs, as the aggregation would consume more power than it would normally consume.

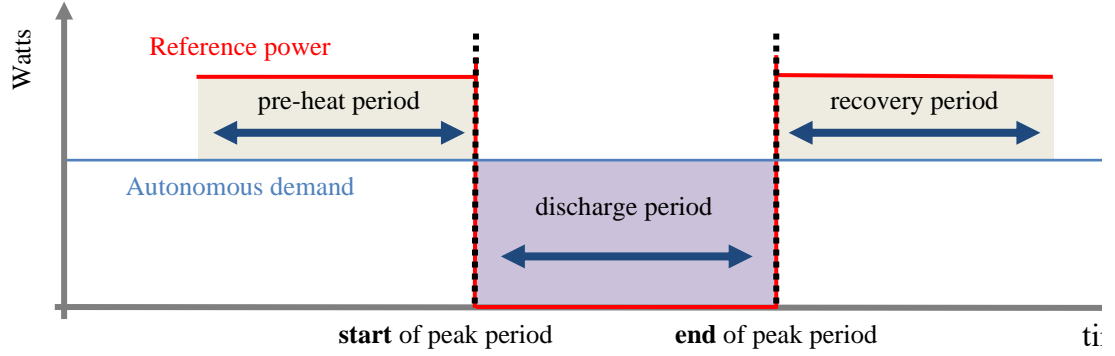


Figure 5.4: DLC strategy.

The pre-heat period main objective is to increase the stored energy in the aggregation as close to the maximum value. The stored energy is represented by the State of Charge (SoC) of the devices. The SoC of an individual TCL is interpreted as:

$$SoC_i(t) = \max\left(\frac{T_i(t) - T_{i,min}}{T_{i,max} - T_{i,min}}, 0\right) \times 100\% \quad (5.14)$$

where  $T_i(t)$  is the TCL's storage medium (water, room, brick) temperature,  $T_{i,min}$  and  $T_{i,max}$  are the lower and upper bounds of the temperature hysteresis band.  $SoC_i(t)$  is the ratio of energy contained within the medium relative to the energy of a fully charged TCL ( $T_i = T_{i,max}$ ).  $SoC_i(t)$  is set to 0% when  $T_i(t) < T_{i,min}$  because there is no more energy stored in the TCL that can be used for DLC without impacting end-user comfort. The value of  $SoC$  at the aggregation level is calculated as:

$$SoC_{agg}(t) = \frac{1}{N} \sum_{i=1}^N SoC_i(t) \quad (5.15)$$

where  $N$  is the number of TCLs in the aggregation.

Control is released when  $SoC_{agg,DLC}(t) \geq SoC_{agg,Autonomous}(t)$ . This condition ensures that, when the control is released, the aggregation will not produce a peak above the

autonomous demand since the TCLs will have the same or more energy stored than without control. Two values for the minimum temperature threshold were analyzed during the peak hours:

Scenario 1: defined by the autonomous behavior of the thermostat as:

$$T_{min} = T_{set} - T_{hb}/2 \quad (5.16)$$

where  $T_{set}$  and  $T_{hb}$  are the thermostat setpoint and hysteresis band respectively ( $^{\circ}\text{C}$ ).

Scenario 2:  $T_{min} = 50^{\circ}\text{C}$ . A value of  $50^{\circ}\text{C}$  meets the hot water needs of the average customer [38], [90] and adds a safety factor against the proliferation of bacterial colonies [38], [90], [123].

The lower temperature threshold of  $50^{\circ}\text{C}$  allows the water heaters to be deactivated for a longer time, increasing the available dispatch capacity during the peak period at the expense of reducing the setpoint temperature. Figure 5.6 illustrates the impact of the control actions on the ability of water heaters to deliver hot water. As shown, the DLC program has negligible impact on this ability. The temperature is above  $55^{\circ}\text{C}$  for most of the time in both scenarios, and it never drops below  $45^{\circ}\text{C}$ . However, reducing the setpoint to  $50^{\circ}\text{C}$  increases the time it takes for the water heaters to return to their normal behavior. This raises the payback, and therefore, the time to control it also increases.

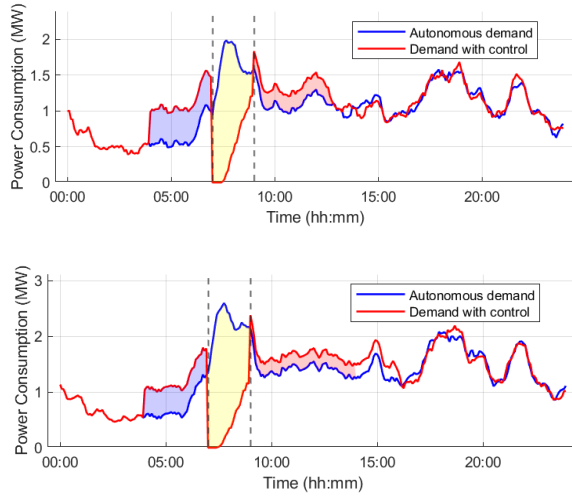


Figure 5.5: Aggregate power demand of 2000 DEWHs with DLC program over 24 hours. Top: DLC with minimum water temperature threshold as defined in equation. (5.16). Bottom: DLC with minimum threshold of 50°C during peak period.

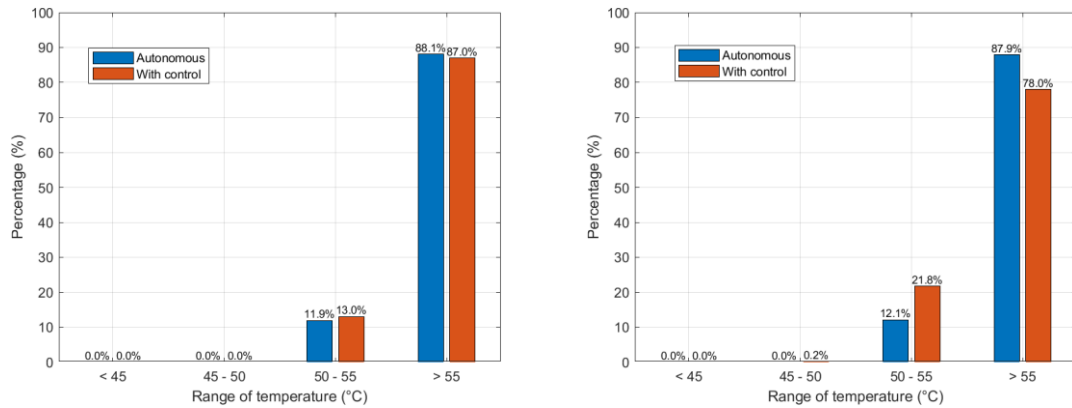


Figure 5.6: Percentage of events in supply temperatures for 2000 DEWHs to deliver hot water under DLC program for 24 hours. Left: DLC with minimum water temperature threshold as defined in equation. (5.16). Right: DLC with minimum threshold of 50°C during peak period.

### **5.3.1 Dispatch capacity estimation of aggregated DEWHs**

SJE plans to deploy 2000 DEWHs as part of their smart grid project [34]. An ensemble of 100 iterations is implemented to provide the probabilistic range of the dispatch capacity for each scenario.

The two scenarios of the DLC program were applied to the autonomous ensemble forecast, resulting in the ensemble forecasts of the demand with control. The difference between the demand with control and the autonomous demand is measured for each iteration of the simulations, creating the regulated demand shown in Figure 5.7. Negative values represent when the demand with control is lower than the autonomous demand.

The probabilistic interval of the regulated power is larger in the first hour and decreases towards the end of the peak period. This happens because the water heaters are turning on to counteract the decrease in the water temperature. Thus, less DEWHs are available to the controller after the first hour. Figure 5.8 shows a boxplot of the dispatchable energy capacity during peak hours. Scenario 2 exhibits a possible 1 MWh of additional capacity.

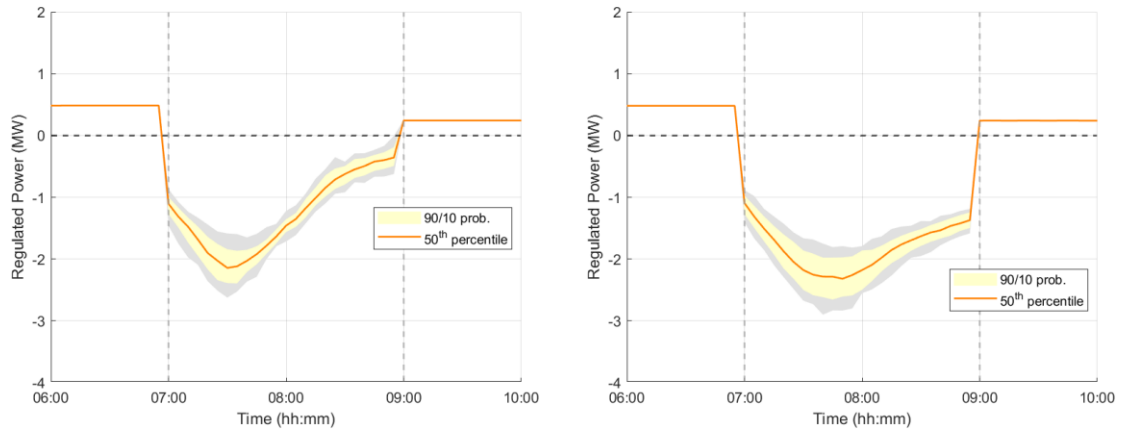


Figure 5.7: Probabilistic forecast of the regulated power of 2000 DEWHs. Left: DLC with minimum water temperature threshold as defined in equation. (5.16). Right: DLC with minimum threshold of 50°C during peak period.

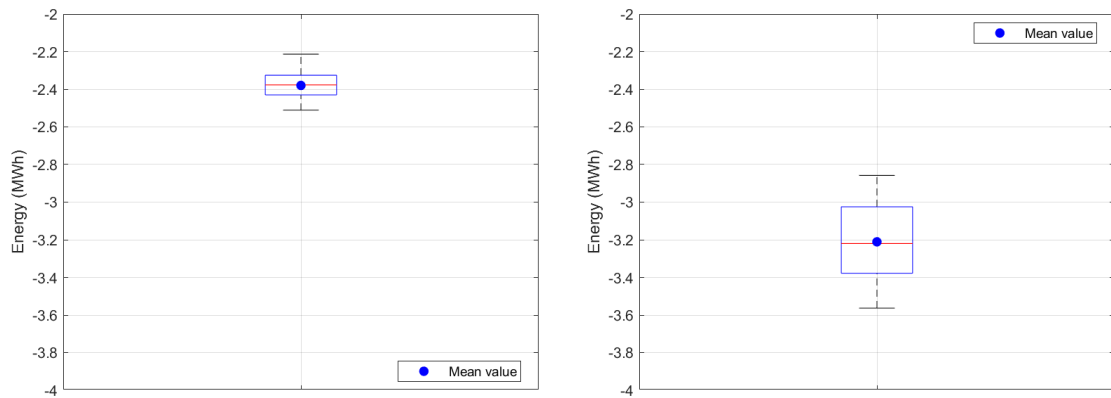


Figure 5.8: Energy capacity of 2000 DEWHs with DLC program. Left: DLC with minimum water temperature threshold as defined in equation. (5.16) ( $\bar{x} = -2.389$  MWh,  $S_x = 0.0633$  MWh,  $E = 0.519\%$ ). Right: DLC with minimum threshold of 50°C during peak period ( $\bar{x} = -3.21$  MWh,  $S_x = 0.1896$  MWh,  $E = 1.157\%$ ).

## 5.4 Dispatch capacity estimation of aggregated EBHs

The advanced setpoint strategy described in section 5.2 was applied to an aggregation of 200 EBHs, as SJE plans to install approximately 200 controllers onto customer's existing electric heaters [34]. Figure 5.9 shows the effects of the strategy on the aggregation assuming peak time from 7 to 9 a.m.

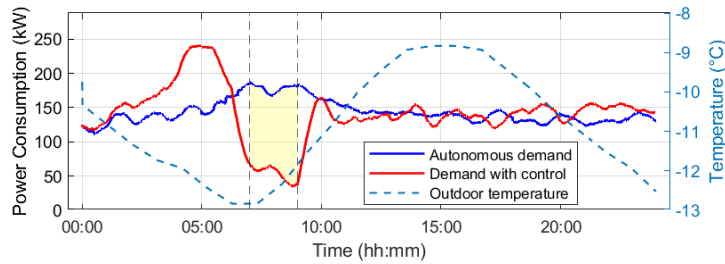


Figure 5.9: Aggregate power demand of 200 EBHs with DR schedule over 24 hours.

Figure 5.10 shows the impact of the control actions on the room temperatures. There is a minor impact, as can be seen by the light increase in the temperature deviation with respect to the customer's desired temperature.

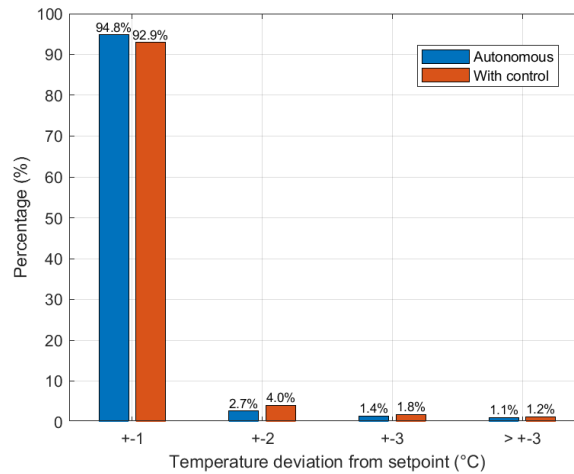


Figure 5.10: Percentage of room temperatures deviation from thermostats setpoints.

Figure 5.11 illustrates the outdoor temperature range used as input to the aggregated EBHs model to provide a dispatch capacity forecast for a day. The outdoor temperature is taken from the weather forecaster<sup>1</sup> plus an error with a random normal distribution with mean of  $-0.23^{\circ}\text{C}$ , standard deviation of  $1.82^{\circ}\text{C}$ . This error distribution was obtained by measuring the difference between the actual and forecasted outdoor air temperature from December 2020 to March 2021. Figure 5.12 shows the regulated demand together with a boxplot of the dispatchable energy capacity. An ensemble of 100 iterations of the setpoint control strategy is applied with the same probability applied to each iteration.

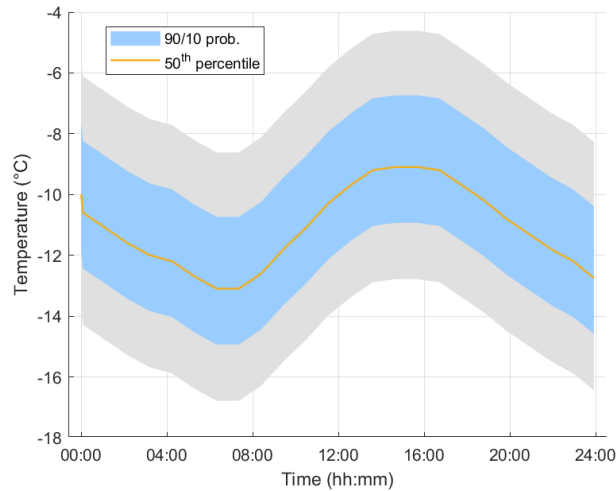


Figure 5.11: Outdoor temperature range.

The small number of EBHs used in this scenario increases the uncertainties of the probabilistic output. As more devices are added to the program, the impact of each device at the aggregation will decrease and the probabilistic dispatch capacity forecast will be narrower.

---

<https://weather.amec.com/AWx2><sup>1</sup>

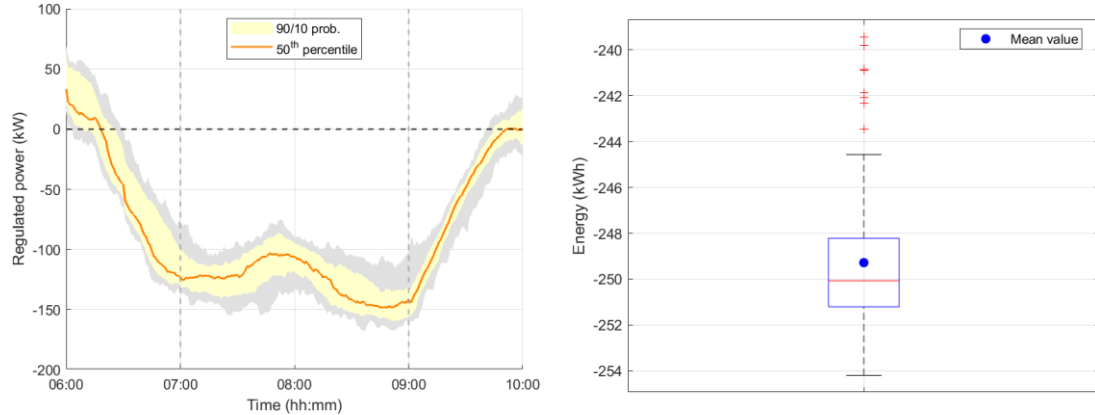


Figure 5.12: Left: Probabilistic forecast of the regulated power of 200 EBHs. Right: Energy capacity ( $\bar{x} = -0.245$  MWh,  $S_x = 0.0044$  MWh,  $E = 0.39\%$ ).

## 5.5 Dispatch capacity estimation of aggregated ETSs

The same strategy depicted in Figure 5.4 together with the DTFC algorithm is used in the aggregation of ETSs. The high thermal inertia of brick-core ETS allow the control to turn them off for prolonged periods of time without affecting the available heat supply. It also means that the temperature of the bricks will increase/decrease slowly. Figure 5.13 shows the aggregate power demand of 50 ETSs with and without DLC assuming peak period from 7 a.m. to 9 a.m. This number of devices are planned to be deployed by SJE [34]. It should be noted that there is no control after the end of the peak period. The temperature of the bricks is still high enough, so no immediate payback is created. Although, a small peak above the autonomous demand appears around the 18<sup>th</sup> hour. This can be interpreted as a delayed payback, due to the high thermal inertia of ETSs. Figure 5.14 demonstrates the small impact of the control actions on the ability of the ETSs to store enough heat on their bricks.

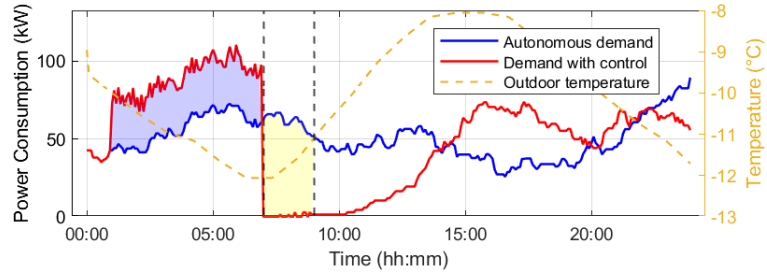


Figure 5.13: Aggregate power demand of 50 ETSs with DLC over 24 hours.

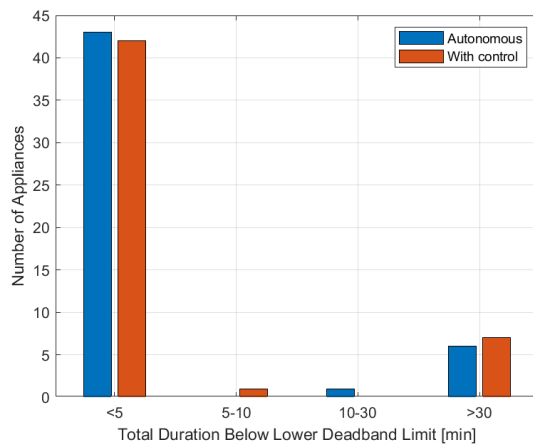


Figure 5.14: Duration for which the bricks temperature is below the minimum threshold.

The probabilistic regulated power and the boxplot of the dispatchable energy capacity of an aggregation of ETSs is illustrated in Figure 5.15. It consists of 100 iterations of the DLC strategy depicted in Figure 5.4 using the outdoor temperature profile shown in Figure 5.11. Since this amount of ETSs is small, the behavior of a single device has a high influence at the aggregation level. This adds more uncertainties about the dispatch capacity forecast, which is reflected in a wider range of possible values.

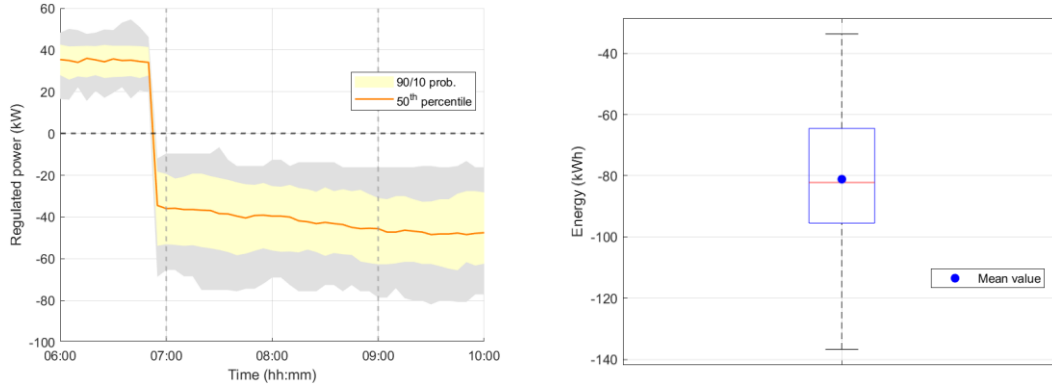


Figure 5.15: Left: Probabilistic forecast of the regulated power of 50 ETSs. Right: Energy capacity ( $\bar{x} = -0.08$  MWh,  $S_x = 0.021$  MWh,  $E = 4.76\%$ ).

## 5.6 Planning tool

The simulated models and the DLC strategies were used to implement a planning tool that utilities and/or aggregators can use to forecast the dispatch capacity of homogeneous aggregations of DEWHs, EBHs or ETSs. This tool was developed in MATLAB and comprises a user interface (Figure 5.16) permitting to modify the characteristics of the aggregation. The input parameters considered for the model include: aggregation size, setpoint temperatures, rated powers, start hour of the preheating period, start and end hours of the forecasted peak period, room ambient temperatures (DEWHs), tank volumes (DEWHs), outdoor temperature to estimate inlet water temperature (DEWHs) or as a parameter (EBHs, ETSs), and the number of iterations the probabilistic forecaster should perform. The outputs include a sample iteration of the autonomous demand of the aggregation, the demand with control and the corresponding regulated power. It also outputs the probabilistic forecast (Figure 5.17), indicating the 10<sup>th</sup> and 90<sup>th</sup> percentiles.

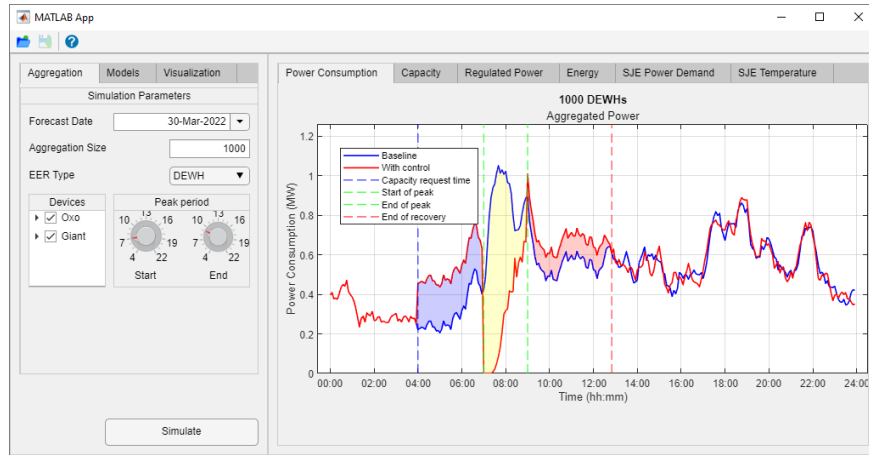


Figure 5.16: User interface using MATLAB showing an iteration result of the power consumption for an aggregation of 1000 DEWHs.

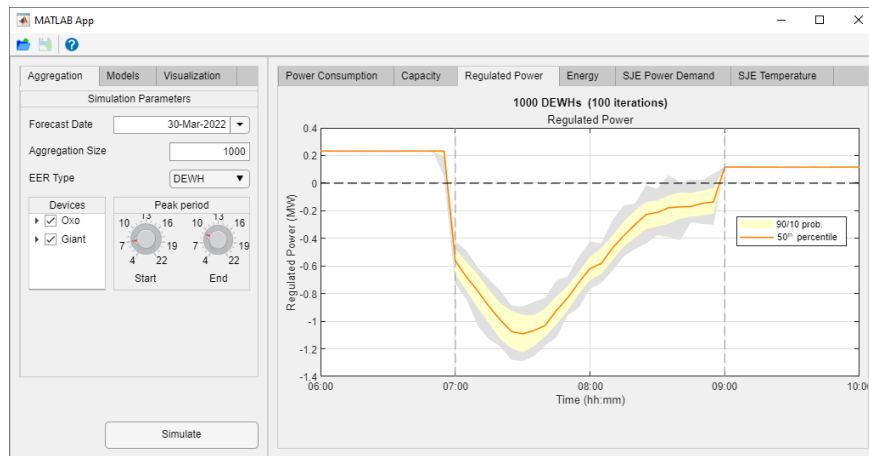


Figure 5.17: User interface and probabilistic dispatch capacity forecast results for an aggregation of 1000 DEWHs.

## 5.7 Chapter Conclusions

The application of the proposed modifications to the DLC algorithm for DEWHs control increased the dispatchable capacity at the expense of increasing the payback effect and the time needed to control it. With this approach, an aggregation of 2000 DEWH was able to provide an average dispatch capacity of 1.2 MW (30% reduction of the non-controlled

aggregated demand) during a two-hours-long peak period (from 7 a.m. to 9 a.m.) with negligible impact on user comfort.

The proposed approach, applied to an aggregation of 50 ETSs, produced a dispatch capacity above 45 kW (85% aggregated demand reduction) during peak hours with a small impact on the devices ability to store heat and therefore on user comfort.

The proposed set of rules to the Advance DR strategy applied to an aggregation of 200 EBHs increased the dispatch capacity during peak hours above 120 kW on average (60% aggregated demand reduction) in the simulated scenario. Simulations showed minor impact on user comfort. Although preheating load shifting strategy produced a reduction in the payback effect, the later depends on the setting of temperature thresholds during peak period so a compromise should be found between desired dispatch capacity increase and manageable payback effect.

## 6 Conclusions and Future Work

This thesis proposes a probabilistic dispatch capacity forecast of aggregated DERs. The proposed framework includes the short-term forecasting of aggregated load demand and a scheme to control the aggregated loads to increase their dispatchable capacity. The proposed strategy for aggregate DERs control consists of a modified DLC strategy and a modified Advanced DR setpoint control schedule.

The evaluation of the proposed methods in this study is based on the use of simulated load models to replicate and estimate the power consumption of different DERs and homogeneous aggregations. The use of simulated load models provides a solution regarding the lack of actual data and allows the number of simulated devices to be increased to a larger population. This approach also permits the systematic monitoring of the state of each device and, consequently, the tracking of end-user comfort.

The proposed short-term probabilistic dispatch capacity forecast takes into consideration uncertainties in the inputs, models parameters and stochastic user behavior. These uncertainties are used to estimate probable loads of homogeneous DER aggregations for one-day simulation scenarios, with peak periods defined from 7 a.m. to 9 a.m.

MC experiments were designed to evaluate the suitability of the aggregated DERs control approach and the 24 hours ahead dispatch capacity forecast of homogeneous aggregations of DEWHs, EBHs and ETSs. The simulation results showed that for an aggregation of 2000 DEWHs the average dispatch capacity estimation is -2.389 MWh during peak periods, with 0.519 percentage error. The dispatch capacity prediction for an aggregation of 200 EBHs is -245 kWh with 0.39 percentage error. Finally, for an aggregation of 50

ETSSs, the predicted average dispatch capacity during peak period is -80 kWh, with 4.76 percentage error. These results confirmed the feasibility of proposed framework to forecast dispatch capacity and the efficiency of planned control strategies to increase dispatch capacity during load peak period.

The payback effect, an inevitable consequence of the control actions applied during peak period, depends on the setting of temperature thresholds. The combination of the proposed load shifting mechanisms and the control strategies allowed the increment of the dispatchable capacity by setting lower temperature thresholds during the peak period. This action also increased the payback effect both in magnitude and duration. Therefore, there exists a tradeoff between increasing dispatch capacity and manageable payback effect.

The evaluation of end-user comfort was adapted to the specific usage of each type of DER. Water supply temperatures were above 45°C in all DEWHs simulation scenarios, and only in 0.2% of the simulated events the temperatures were below the minimum setpoint of 50°C. The Advanced DR setpoint control schedule implemented in EBHs aggregation caused a room temperature deviation of 1°C or less from thermostats setpoints in 92.9% of the samples, and only 1.2% showed deviations of more than 3°C. The experiments with ETSSs showed a low effect of the control actions on the ability of these devices to store enough heat in their bricks, as 84% of devices kept their bricks temperature above the minimum threshold for 99.6% of the time. The impact on end-user comfort of the proposed control strategies can be accepted as low for all considered DERs according to the proposed methodology for its evaluation.

The proposed algorithms were implemented in a planning tool to forecast the dispatch capacity of homogeneous aggregations of DEWHs, EBHs and ETSs. The forecasting methods and algorithms of this tool are relevant not only for SJE scenarios but also for any LDN that is implementing peak shaving and needs to optimize the contribution of different aggregators to curtail the peak load demand. The short-term probability forecast produces a range of values of dispatch capacity that gives the power system operator the possibilities to reduce the power demand during the peak period without affecting system stability even in the worst-case scenario.

## **6.1 Future Work**

The main directions of future work are:

- Compare the forecasted power consumption of the models with actual data obtained from devices deployed as part of SJE smart grid program and fine-tune the models.
- Expand the analysis to other DERs involved in SJE project, such as heat pumps and electric vehicles.
- Analyse the forecast of dispatch capacity of DER aggregator with other control algorithms that require less information from the devices.

## Bibliography

- [1] H. Ritchie and M. Roser, “Energy,” *Our World In Data*, 2020, [Online]. Available: <https://ourworldindata.org/energy>.
- [2] M. S. Hossain, N. A. Madloul, N. A. Rahim, J. Selvaraj, A. K. Pandey, and A. F. Khan, “Role of smart grid in renewable energy: An overview,” *Renewable and Sustainable Energy Reviews*, vol. 60. Elsevier Ltd, pp. 1168–1184, Jul. 01, 2016, doi: 10.1016/j.rser.2015.09.098.
- [3] D. B. Richardson, “Electric vehicles and the electric grid: A review of modeling approaches, Impacts, and renewable energy integration,” *Renew. Sustain. Energy Rev.*, vol. 19, pp. 247–254, 2013, doi: 10.1016/J.RSER.2012.11.042.
- [4] X. Gong, E. C. Guerra, and J. Cardenas Barrera, “Aggregated load forecast and control for creating alternative power system resources using thermostatically controlled loads,” University of New Brunswick., 2021.
- [5] M. Mallette and G. Venkataramanan, “The role of plug-in hybrid electric vehicles in demand response and beyond,” *2010 IEEE PES Transm. Distrib. Conf. Expo. Smart Solut. a Chang. World*, 2010, doi: 10.1109/TDC.2010.5484613.
- [6] T. Okazaki, “Electric thermal energy storage and advantage of rotating heater having synchronous inertia,” *Renew. Energy*, vol. 151, pp. 563–574, May 2020, doi: 10.1016/j.renene.2019.11.051.
- [7] E. Bertoli, T. Goodson, P. Henriot, and H. Kim, “Demand Response,” IEA, Paris, Nov. 2021. [Online]. Available: <https://www.iea.org/reports/demand-response>.
- [8] M. E. El-Hawary, “The smart grid - State-of-the-art and future trends,” *Electr. Power Components Syst.*, vol. 42, no. 3–4, pp. 239–250, Mar. 2014, doi: 10.1080/15325008.2013.868558.
- [9] G. Le Ray and P. Pinson, “The ethical smart grid: Enabling a fruitful and long-lasting relationship between utilities and customers,” *Energy Policy*, vol. 140, p. 111258, May 2020, doi: 10.1016/j.enpol.2020.111258.
- [10] P. Palensky and D. Dietrich, “Demand side management: Demand response, intelligent energy systems, and smart loads,” *IEEE Trans. Ind. Informatics*, vol. 7, no. 3, pp. 381–388, Aug. 2011, doi: 10.1109/TII.2011.2158841.
- [11] A. Arteconi, N. J. Hewitt, and F. Polonara, “State of the art of thermal storage for demand-side management,” *Appl. Energy*, vol. 93, pp. 371–389, May 2012, doi: 10.1016/j.apenergy.2011.12.045.
- [12] V. S. K. M. Balijepalli, V. Pradhan, S. A. Khaparde, and R. M. Shereef, “Review of demand response under smart grid paradigm,” in *2011 IEEE PES International Conference on Innovative Smart Grid Technologies-India, ISGT India 2011*, 2011, pp. 236–243, doi: 10.1109/ISET-India.2011.6145388.
- [13] E. Guelpa and V. Verda, “Demand response and other demand side management techniques for district heating: A review,” *Energy*, vol. 219, p. 119440, Mar. 2021, doi: 10.1016/J.ENERGY.2020.119440.
- [14] Y. Wang and H. Nazaripouya, “Demand-side management in micro-grids and distribution systems: Handling system uncertainties and scalabilities,” *Class. Recent Asp. Power Syst. Optim.*, pp. 361–387, Jun. 2018, doi: 10.1016/B978-0-12-812441-3.00013-6.

- [15] M. Diekerhof, A. Monti, and S. Schwarz, “Demand-side management- recent aspects and challenges of optimization for an efficient and robust demand-side management,” *Class. Recent Asp. Power Syst. Optim.*, pp. 331–360, Jun. 2018, doi: 10.1016/B978-0-12-812441-3.00012-4.
- [16] G. Strbac, “Demand side management: Benefits and challenges,” *Energy Policy*, vol. 36, no. 12, pp. 4419–4426, Dec. 2008, doi: 10.1016/j.enpol.2008.09.030.
- [17] E. M. Wanjiru, S. M. Sichilalu, and X. Xia, “Model predictive control of heat pump water heater-instantaneous shower powered with integrated renewable-grid energy systems,” *Appl. Energy*, vol. 204, pp. 1333–1346, Oct. 2017, doi: 10.1016/j.apenergy.2017.05.033.
- [18] A. M. Carreiro, H. M. Jorge, and C. H. Antunes, “Energy management systems aggregators: A literature survey,” *Renewable and Sustainable Energy Reviews*, vol. 73. Elsevier Ltd, pp. 1160–1172, Jun. 01, 2017, doi: 10.1016/j.rser.2017.01.179.
- [19] B. Daryanian and R. E. Bohn, “Sizing of Electric Thermal Storage Under Real Time Pricing,” *IEEE Trans. Power Syst.*, vol. 8, no. 1, pp. 35–43, 1993, doi: 10.1109/59.221246.
- [20] S. Wong, N. Lévesque, V. Delisle, A. Gagné, and L. P. Proulx, “Using the thermal energy storage potential of residential homes for ToU rate savings and demand response,” *2017 5th IEEE Int. Conf. Smart Energy Grid Eng. SEGE 2017*, pp. 223–228, 2017, doi: 10.1109/SEGE.2017.8052802.
- [21] S. Dery, A. Wadhwa, S. Wong, and L. P. Proulx, “Real-World Implementation of Residential Thermostat Control for DR,” *Can. Conf. Electr. Comput. Eng.*, vol. 2018-May, Aug. 2018, doi: 10.1109/CCECE.2018.8447742.
- [22] N. Ruiz, B. Claessens, J. Jimeno, J. A. López, and D. Six, “Residential load forecasting under a demand response program based on economic incentives,” *Int. Trans. Electr. Energy Syst.*, vol. 25, no. 8, pp. 1436–1451, Aug. 2015, doi: 10.1002/etep.1905.
- [23] M. Uddin, M. F. Romlie, M. F. Abdullah, S. Abd Halim, A. H. Abu Bakar, and T. Chia Kwang, “A review on peak load shaving strategies,” *Renewable and Sustainable Energy Reviews*, vol. 82. Elsevier Ltd, pp. 3323–3332, Feb. 01, 2018, doi: 10.1016/j.rser.2017.10.056.
- [24] K. Y. Huang and Y. C. Huang, “Integrating direct load control with interruptible load management to provide instantaneous reserves for ancillary services,” *IEEE Trans. Power Syst.*, vol. 19, no. 3, pp. 1626–1634, Aug. 2004, doi: 10.1109/TPWRS.2004.831705.
- [25] R. Henriquez, G. Wenzel, D. E. Olivares, and M. Negrete-Pincetic, “Participation of demand response aggregators in electricity markets: Optimal portfolio management,” *IEEE Trans. Smart Grid*, vol. 9, no. 5, pp. 4861–4871, Sep. 2018, doi: 10.1109/TSG.2017.2673783.
- [26] N. Lu and Y. Zhang, “Design considerations of a centralized load controller using thermostatically controlled appliances for continuous regulation reserves,” *IEEE Trans. Smart Grid*, vol. 4, no. 2, pp. 914–921, 2013, doi: 10.1109/TSG.2012.2222944.
- [27] M. Safdar, M. Ahmad, A. Hussain, and M. Lehtonen, “Optimized residential load

- scheduling under user defined constraints in a real-time tariff paradigm,” in *2016 17th International Scientific Conference on Electric Power Engineering (EPE)*, Jul. 2016, pp. 1–6, doi: 10.1109/EPE.2016.7521798.
- [28] H. Salehfar and A. Wehbe, “Direct control of residential water heater loads to reduce power system distribution losses,” *Proc. IEEE Power Eng. Soc. Transm. Distrib. Conf.*, vol. 3, no. WINTER MEETING, pp. 1455–1460, 2001, doi: 10.1109/PESW.2001.917319.
- [29] J. Shen, C. Jiang, and B. Li, “Controllable Load Management Approaches in Smart Grids,” *Energies*, vol. 8, no. 10, pp. 11187–11202, Oct. 2015, doi: 10.3390/en81011187.
- [30] J. L. Mathieu, S. Koch, and D. S. Callaway, “State estimation and control of electric loads to manage real-time energy imbalance,” *IEEE Trans. Power Syst.*, vol. 28, no. 1, pp. 430–440, 2013, doi: 10.1109/TPWRS.2012.2204074.
- [31] S. A. Pourmousavi, S. N. Patrick, and M. H. Nehrir, “Real-time demand response through aggregate electric water heaters for load shifting and balancing wind generation,” *IEEE Trans. Smart Grid*, vol. 5, no. 2, pp. 769–778, Mar. 2014, doi: 10.1109/TSG.2013.2290084.
- [32] O. Ayan and B. Turkey, “Domestic electrical load management in smart grids and classification of residential loads,” in *2018 5th International Conference on Electrical and Electronics Engineering, ICEEE 2018*, Jun. 2018, pp. 279–283, doi: 10.1109/ICEEE2.2018.8391346.
- [33] A. A. Pardasani Yitian Hu Jennifer Veitch, G. R. Newsham, A. Pardasani, and Y. V. Hu, “Demand Control of Baseboard Heaters Using Connected Thermostats: Lessons Learned from a 567-Home Pilot Study,” *ASHRAE Trans.*, vol. 126, pp. 12–20, 2020.
- [34] “Smart Energy Project | Saint John Energy.”  
<https://www.sjenergy.com/pages/smart-grid>.
- [35] A. Brooks, E. Lu, D. Reicher, C. Spirakis, and B. Weihl, “Demand dispatch,” *IEEE Power Energy Mag.*, vol. 8, no. 3, pp. 20–29, May 2010, doi: 10.1109/MPE.2010.936349.
- [36] M. Shad, A. Momeni, R. Errouissi, C. P. Diduch, M. E. Kaye, and Liuchen Chang, “Identification and Estimation for Electric Water Heaters in Direct Load Control Programs,” *IEEE Trans. Smart Grid*, vol. 8, no. 2, pp. 947–955, 2017, doi: 10.1109/TSG.2015.2492950.
- [37] M. A. Z. Alvarez, K. Agbossou, A. Cardenas, S. Kelouwani, and L. Boulon, “Demand Response Strategy Applied to Residential Electric Water Heaters Using Dynamic Programming and K-Means Clustering,” *IEEE Trans. Sustain. Energy*, vol. 11, no. 1, pp. 524–533, Jan. 2020, doi: 10.1109/TSTE.2019.2897288.
- [38] A. Moreau, “Control strategy for domestic water heaters during peak periods and its impact on the demand for electricity,” in *Energy Procedia*, Jan. 2011, vol. 12, pp. 1074–1082, doi: 10.1016/j.egypro.2011.10.140.
- [39] E. Vrettos, “Control of residential and commercial loads for power system ancillary services,” ETH Zurich, 2016.
- [40] Y. Wang, D. Gan, M. Sun, N. Zhang, Z. Lu, and C. Kang, “Probabilistic individual load forecasting using pinball loss guided LSTM,” *Appl. Energy*, vol. 235, pp. 10–

- 20, Feb. 2019, doi: 10.1016/j.apenergy.2018.10.078.
- [41] T. Hong and S. Fan, “Probabilistic electric load forecasting: A tutorial review,” *Int. J. Forecast.*, vol. 32, no. 3, pp. 914–938, Jul. 2016, doi: 10.1016/j.ijforecast.2015.11.011.
- [42] C. Kuster, Y. Rezgui, and M. Mourshed, “Electrical load forecasting models: A critical systematic review,” *Sustain. Cities Soc.*, vol. 35, pp. 257–270, Nov. 2017, doi: 10.1016/J.SCS.2017.08.009.
- [43] M. Shaad, R. Errouissi, C. P. Diduch, M. E. Kaye, and L. Chang, “Aggregate load forecast with payback model of the electric water heaters for a direct load control program,” in *Proceedings - 2014 Electrical Power and Energy Conference, EPEC 2014*, Feb. 2014, pp. 214–219, doi: 10.1109/EPEC.2014.13.
- [44] M. Vlachopoulou, G. Chin, J. C. J. C. Fuller, S. Lu, and K. Kalsi, “Model for aggregated water heater load using dynamic bayesian networks,” in *Proceedings of the International Conference on Data Science (ICDATA)*, 2012, p. 1.
- [45] X. Gong, J. L. Cardenas-Barrera, E. Castillo-Guerra, B. Cao, S. A. Saleh, and L. Chang, “Bottom-Up Load Forecasting with Markov-Based Error Reduction Method for Aggregated Domestic Electric Water Heaters,” *IEEE Trans. Ind. Appl.*, vol. 55, no. 6, pp. 6401–6413, 2019, doi: 10.1109/TIA.2019.2936330.
- [46] T. Januschowski *et al.*, “Criteria for classifying forecasting methods,” *Int. J. Forecast.*, vol. 36, no. 1, pp. 167–177, Jan. 2020, doi: 10.1016/J.IJFORECAST.2019.05.008.
- [47] L. Gelažanskas and K. A. A. Gamage, “Forecasting hot water consumption in residential houses,” *Energies*, vol. 8, no. 11, pp. 12702–12717, 2015, doi: 10.3390/en8112336.
- [48] D. H. Tungadio and Y. Sun, “Load frequency controllers considering renewable energy integration in power system,” *Energy Reports*, vol. 5, pp. 436–453, 2019, doi: 10.1016/j.egyr.2019.04.003.
- [49] A. Delorme-Costil and J. J. Bezian, “Forecasting domestic hot water demand in residential house using artificial neural networks,” in *Proceedings - 16th IEEE International Conference on Machine Learning and Applications, ICMLA 2017*, 2017, vol. 2017-Decem, pp. 467–472, doi: 10.1109/ICMLA.2017.0-117.
- [50] A. J. Landgraf, “An ensemble approach to GEFCom2017 probabilistic load forecasting,” *Int. J. Forecast.*, vol. 35, no. 4, pp. 1432–1438, Oct. 2019, doi: 10.1016/J.IJFORECAST.2019.02.003.
- [51] Z. Broka, J. Kozadajevs, A. Sauhats, D. P. Finn, and W. J. N. N. Turner, “Modelling residential heat demand supplied by a local smart electric thermal storage system,” in *2016 57th International Scientific Conference on Power and Electrical Engineering of Riga Technical University (RTU CON)*, 2016, pp. 1–8, doi: 10.1109/RTU CON.2016.7763128.
- [52] B. Liu, J. R. Lund, S. Liao, X. Jin, L. Liu, and C. Cheng, “Optimal power peak shaving using hydropower to complement wind and solar power uncertainty,” *Energy Convers. Manag.*, vol. 209, Apr. 2020, doi: 10.1016/j.enconman.2020.112628.
- [53] R. Errouissi, J. Cardenas-Barrera, J. Meng, E. Castillo-Guerra, X. Gong, and L. Chang, “Bootstrap prediction interval estimation for wind speed forecasting,” in

- 2015 IEEE Energy Conversion Congress and Exposition, ECCE 2015, Oct. 2015, pp. 1919–1924, doi: 10.1109/ECCE.2015.7309931.
- [54] M. J. Ritchie, J. A. A. Engelbrecht, and M. J. Booysen, “A probabilistic hot water usage model and simulator for use in residential energy management,” *Energy Build.*, vol. 235, p. 110727, Mar. 2021, doi: 10.1016/J.ENBUILD.2021.110727.
- [55] N. H. Tehrani and P. Wang, “Probabilistic estimation of plug-in electric vehicles charging load profile,” *Electr. Power Syst. Res.*, vol. 124, pp. 133–143, Jul. 2015, doi: 10.1016/J.EPSR.2015.03.010.
- [56] Q. Chang *et al.*, “Probabilistic Load Forecasting via Point Forecast Feature Integration,” in *2019 IEEE PES Innovative Smart Grid Technologies Asia, ISGT 2019*, May 2019, pp. 99–104, doi: 10.1109/ISGT-Asia.2019.8881627.
- [57] C. A. Correa-Florez, A. Michiorri, and G. Kariniotakis, “Robust optimization for day-ahead market participation of smart-home aggregators,” *Appl. Energy*, vol. 229, pp. 433–445, Nov. 2018, doi: 10.1016/j.apenergy.2018.07.120.
- [58] G. R. Aghajani, H. A. Shayanfar, and H. Shayeghi, “Demand side management in a smart micro-grid in the presence of renewable generation and demand response,” *Energy*, vol. 126, pp. 622–637, May 2017, doi: 10.1016/j.energy.2017.03.051.
- [59] M. A. Zu, “Electric Water Heaters Using Dynamic Programming and K-Means Clustering,” *IEEE Trans. Sustain. Energy*, vol. 11, no. 1, pp. 524–533, 2020.
- [60] L. Paull, H. Li, and L. Chang, “A novel domestic electric water heater model for a multi-objective demand side management program,” *Electr. Power Syst. Res.*, vol. 80, pp. 1446–1451, 2010, doi: 10.1016/j.epr.2010.06.013.
- [61] T. Logenthiran, D. Srinivasan, and T. Z. Shun, “Demand side management in smart grid using heuristic optimization,” *IEEE Trans. Smart Grid*, vol. 3, no. 3, pp. 1244–1252, 2012, doi: 10.1109/TSG.2012.2195686.
- [62] J. A. Candanedo, V. R. Dehkordi, A. Saberi-Derakhtenjani, and A. K. Athienitis, “Near-optimal transition between temperature setpoints for peak load reduction in small buildings,” *Energy Build.*, vol. 87, pp. 123–133, Jan. 2015, doi: 10.1016/J.ENBUILD.2014.11.021.
- [63] L. Handfield, H. Nesreddine, and C. Le Bel, “Power Demand of Programmable Thermostats with a Built-in Pick-up Algorithm for Electric Baseboard Heaters,” 2006.
- [64] J. Ikäheimo, C. Evens, and S. Kärkkäinen, “DER Aggregator business: the Finnish case,” *Tech. Res. Cent. Finl. Espoo, Finl.*, p. 39, 2010.
- [65] N. Ruiz, I. Cobelo, and J. Oyarzabal, “A direct load control model for virtual power plant management,” *IEEE Trans. Power Syst.*, vol. 24, no. 2, pp. 959–966, 2009, doi: 10.1109/TPWRS.2009.2016607.
- [66] L. Herre, S. Kazemi, and L. Söder, “Quantifying flexibility of load aggregations: impact of communication constraints on reserve capacity,” *IET Gener. Transm. & Distrib.*, vol. 14, no. 22, pp. 5211–5218, 2020.
- [67] C. Pang, M. Kezunovic, and M. Ehsani, “Demand side management by using electric vehicles as Distributed Energy Resources,” in *2012 IEEE International Electric Vehicle Conference*, Mar. 2012, pp. 1–7, doi: 10.1109/IEVC.2012.6183273.
- [68] C. Diduch, M. Shaad, R. Errouissi, M. E. Kaye, J. Meng, and L. Chang,

- “Aggregated domestic electric water heater control - Building on smart grid infrastructure,” in *Conference Proceedings - 2012 IEEE 7th International Power Electronics and Motion Control Conference - ECCE Asia, IPEMC 2012*, Jun. 2012, vol. 1, pp. 128–135, doi: 10.1109/IPEMC.2012.6258873.
- [69] J. Hu, J. Cao, J. M. Guerrero, T. Yong, and J. Yu, “Improving Frequency Stability Based on Distributed Control of Multiple Load Aggregators,” *IEEE Trans. Smart Grid*, vol. 8, no. 4, pp. 1553–1567, Jul. 2017, doi: 10.1109/TSG.2015.2491340.
- [70] M. Shaad, A. Momeni, C. P. Diduch, M. E. Kaye, and L. Chang, “Forecasting the power consumption of a single domestic electric water heater for a direct load control program,” in *Canadian Conference on Electrical and Computer Engineering*, May 2015, pp. 1550–1555, doi: 10.1109/CCECE.2015.7129511.
- [71] F. Wang *et al.*, “Smart households’ aggregated capacity forecasting for load aggregators under incentive-based demand response programs,” *IEEE Trans. Ind. Appl.*, vol. 56, no. 2, pp. 1086–1097, Mar. 2020, doi: 10.1109/TIA.2020.2966426.
- [72] L. Chang, X. Wang, and M. Mao, “Forecast of schedulable capacity for thermostatically controlled loads with big data analysis,” in *2017 IEEE 8th International Symposium on Power Electronics for Distributed Generation Systems (PEDG)*, Jul. 2017, pp. 1–6, doi: 10.1109/PEDG.2017.7972502.
- [73] S. Chapaloglou *et al.*, “Smart energy management algorithm for load smoothing and peak shaving based on load forecasting of an island’s power system,” *Appl. Energy*, vol. 238, pp. 627–642, Mar. 2019, doi: 10.1016/j.apenergy.2019.01.102.
- [74] M. Suresh, P. Maniraj, S. Sundar, T. Logeswaran, and P. Tamilarasu, “Peak time load management in domestic sector,” *Int. J. Innov. Technol. Explor. Eng.*, vol. 9, no. 1, pp. 2761–2763, Nov. 2019, doi: 10.35940/ijitee.A5221.119119.
- [75] T. L. Clarke, “Aggregation of electric water heaters for peak shifting and frequency response services,” Portland State University, 2019.
- [76] S. Ayoub, “Electric water heaters control strategy for providing regulation services and load leveling in electric power systems,” in *2013 IEEE Electrical Power & Energy Conference*, Aug. 2013, pp. 1–6, doi: 10.1109/EPEC.2013.6802972.
- [77] Y. M. Atwa, E. F. El-Saadany, and M. M. Salama, “DSM Approach for Water Heater Control Strategy Utilizing Elman Neural Network,” *2007 IEEE Canada Electr. Power Conf. EPC 2007*, pp. 382–385, 2007, doi: 10.1109/EPC.2007.4520362.
- [78] B. J. Lameris, M. H. Nehrir, and V. Gerez, “Controlling the average residential electric water heater power demand using fuzzy logic,” *Electr. Power Syst. Res.*, vol. 52, no. 3, pp. 267–271, Dec. 1999, doi: 10.1016/S0378-7796(99)00022-X.
- [79] A. Ahmad, N. Javaid, A. Mateen, M. Awais, and Z. A. Khan, “Short-Term Load Forecasting in Smart Grids: An Intelligent Modular Approach,” *Energies*, vol. 12, no. 1, p. 164, Jan. 2019, doi: 10.3390/en12010164.
- [80] C. Guzman, K. Agbossou, and A. Cardenas, “Modeling of residential centralized and baseboard space heating systems,” in *2016 IEEE 25th International Symposium on Industrial Electronics (ISIE)*, Jun. 2016, pp. 726–731, doi: 10.1109/ISIE.2016.7744979.
- [81] M. A. Bregaw, “Modeling, Simulation and Optimization of Residential and Commercial Energy Systems,” Dalhousie University, 2013.

- [82] S. Canada, “Households and the environment: Energy use,” 2011. [Online]. Available: <https://www150.statcan.gc.ca/n1/pub/11-526-s/11-526-s2013002-eng.pdf>.
- [83] J. Khoury, R. Mbayed, G. Salloum, and E. Monmasson, “Modeling of a hybrid domestic solar/electric water heater for hardware implementation,” in *Proceedings of the Mediterranean Electrotechnical Conference - MELECON*, 2014, pp. 560–565, doi: 10.1109/MELCON.2014.6820596.
- [84] M. A. Moffet, F. Sirois, G. Joós, and A. Moreau, “Central electric thermal storage (ETS) heating systems: Impact on customer and distribution system,” in *Proceedings of the IEEE Power Engineering Society Transmission and Distribution Conference*, 2012, pp. 1–7, doi: 10.1109/TDC.2012.6281536.
- [85] P. S. Sauter, B. V. Solanki, C. A. Canizares, K. Bhattacharya, and S. Hohmann, “Electric Thermal Storage System Impact on Northern Communities’ Microgrids,” *IEEE Trans. Smart Grid*, vol. 10, no. 1, pp. 852–863, Jan. 2019, doi: 10.1109/TSG.2017.2754239.
- [86] N. T. Janssen, R. A. Peterson, and R. W. Wies, “Generalized heat flow model of a forced air electric thermal storage heater core,” *J. Therm. Sci. Eng. Appl.*, vol. 9, no. 4, p. 41008, 2017, [Online]. Available: [http://asmedigitalcollection.asme.org/thermalscienceapplication/article-pdf/9/4/041008/6421598/tsea\\_009\\_04\\_041008.pdf](http://asmedigitalcollection.asme.org/thermalscienceapplication/article-pdf/9/4/041008/6421598/tsea_009_04_041008.pdf).
- [87] W. Devia, K. Agbossou, and A. Cardenas, “An evolutionary approach to modeling and control of space heating and thermal storage systems,” *Energy Build.*, vol. 234, p. 110674, Mar. 2021, doi: 10.1016/j.enbuild.2020.110674.
- [88] S. Xiang, L. Chang, B. Cao, Y. He, and C. Zhang, “A novel domestic electric water heater control method,” *IEEE Trans. Smart Grid*, vol. 11, no. 4, pp. 3246–3256, 2019.
- [89] J. A. A. Engelbrecht, M. J. Ritchie, and M. J. Booysen, “Optimal schedule and temperature control of stratified water heaters,” *Energy Sustain. Dev.*, vol. 62, pp. 67–81, Jun. 2021, doi: 10.1016/J.ESD.2021.03.009.
- [90] S. Xiang, “Domestic electric water heater control for peak shaving & frequency control,” University of New Brunswick., 2021.
- [91] M. Fournier, M.-A. Leduc, and G. Nadrault, “Winter demand response using baseboard heaters: achieving substantial demand reduction without sacrificing comfort,” *Proc. ACEEE Summer Study Energy Effic. Build. (Pacific Grove, CA)*, p. 1, 2016.
- [92] H. Nesreddine, J. Bouchard, and A. Laperriere, “Grid disturbance through thermostat setback,” in *Proceedings of the 3rd WSEAS International Conference on Energy Planning, Energy Saving, Environmental Education, EPESE '09, Renewable Energy Sources, RES '09, Waste Management, WWAI '09*, 2009, pp. 102–109, doi: 10.13140/RG.2.2.30166.55361.
- [93] A. Pardasani, M. Armstrong, G. Newsham, and B. Hanson, “Intelligent management of baseboard heaters to level peak demand,” Dec. 2016, doi: 10.1109/EPEC.2016.7771730.
- [94] L. Handfield, H. Nesreddine, and C. Le Bel, “Improved pick-up algorithms for line voltage programmable thermostats,” *WSEAS Trans. Power Syst.*, vol. 1, no. 10, p.

- 1777, 2006.
- [95] J. Xie and T. Hong, “GEFCom2014 probabilistic electric load forecasting: An integrated solution with forecast combination and residual simulation,” *Int. J. Forecast.*, vol. 32, no. 3, pp. 1012–1016, 2016, doi: 10.1016/j.ijforecast.2015.11.005.
- [96] T. Hong, P. Pinson, S. Fan, H. Zareipour, A. Troccoli, and R. J. Hyndman, “Probabilistic energy forecasting: Global Energy Forecasting Competition 2014 and beyond,” *International Journal of Forecasting*, vol. 32, no. 3. Elsevier, pp. 896–913, 2016, doi: 10.1016/j.ijforecast.2016.02.001.
- [97] W. Oberle, “Monte Carlo Simulations: Number of Iterations and Accuracy,” *US Army Res. Lab.*, p. 25, 2015.
- [98] M. Pfeiffer, G. Andersson, and K. Stephan, “Load Control Strategies for Electric Water Heaters with Thermal Stratification,” Citeseer, 2011.
- [99] H. Djamila, “Indoor thermal comfort predictions: Selected issues and trends,” *Renew. Sustain. Energy Rev.*, vol. 74, pp. 569–580, Jul. 2017, doi: 10.1016/J.RSER.2017.02.076.
- [100] R. R. Gonzalez, Y. Nishi, and A. P. Gagge, “Experimental evaluation of standard effective temperature a new biometeorological index of man’s thermal discomfort,” *Int. J. Biometeorol. 1974 181*, vol. 18, no. 1, pp. 1–15, Mar. 1974, doi: 10.1007/BF01450660.
- [101] D. Fiala and G. Havenith, “Modelling Human Heat Transfer and Temperature Regulation,” *Stud. Mechanobiol. Tissue Eng. Biomater.*, vol. 19, pp. 265–302, 2015, doi: 10.1007/8415\_2015\_183.
- [102] G. Brager, M. Fountain, C. Benton, E. A. Arens, and F. Bauman, “A Comparison of Methods for Assessing Thermal Sensation and Acceptability in the Field,” in *Forensic Engineering: Damage Assessments for Residential and Commercial Structures*, 1993, pp. 17–39.
- [103] B. Koelblen, A. Psikuta, A. Bogdan, S. Annaheim, and R. M. Rossi, “Thermal sensation models: a systematic comparison,” *Indoor Air*, vol. 27, no. 3, pp. 680–689, May 2017, doi: 10.1111/INA.12329.
- [104] A. Beizaee, S. Firth, K. Vadodaria, and D. Loveday, “Assessing the ability of PMV model in predicting thermal sensation in naturally ventilated buildings in UK,” Jan. 2012.
- [105] Y. Zhang and R. Zhao, “Overall thermal sensation, acceptability and comfort,” *Build. Environ.*, vol. 43, no. 1, pp. 44–50, Jan. 2008, doi: 10.1016/J.BUILDENV.2006.11.036.
- [106] M. Shaad, A. Momeni, C. P. Diduch, M. Kaye, and L. Chang, “Parameter identification of thermal models for domestic electric water heaters in a direct load control program,” in *2012 25th IEEE Canadian Conference on Electrical and Computer Engineering (CCECE)*, 2012, pp. 1–5.
- [107] Z. Xu, R. Diao, S. Lu, J. Lian, and Y. Zhang, “Modeling of electric water heaters for demand response: A baseline PDE model,” *IEEE Trans. Smart Grid*, vol. 5, no. 5, pp. 2203–2210, Sep. 2014, doi: 10.1109/TSG.2014.2317149.
- [108] D. Fischer, T. Wolf, J. Scherer, and B. Wille-Haussmann, “A stochastic bottom-up model for space heating and domestic hot water load profiles for German

- households,” *Energy Build.*, vol. 124, pp. 120–128, Jul. 2016, doi: 10.1016/j.enbuild.2016.04.069.
- [109] D. S. Parker, P. W. Fairey, and J. D. Lutz, “Estimating daily domestic hot-water use in North American homes,” *ASHRAE Trans*, vol. 121, no. 2, pp. 258–270, 2015.
- [110] R. Hendron and C. Engebrecht, “Building America Research Benchmark Definition: Updated December 2009,” National Renewable Energy Laboratory, 2010. [Online]. Available: [https://digitalscholarship.unlv.edu/sustain\\_pubs/2](https://digitalscholarship.unlv.edu/sustain_pubs/2).
- [111] “Saint John Climate, Weather By Month, Average Temperature (Canada) - Weather Spark.” <https://weatherspark.com/y/27855/Average-Weather-in-Saint-John-Canada-Year-Round>.
- [112] S. Canada, “Saint John, C [Census subdivision], New Brunswick and New Brunswick [Province] (table). Census Profile. 2016 Census.” Ottawa, 2017. [Online]. Available: <https://www12.statcan.gc.ca/census-recensement/2016/dp-pd/prof/index.cfm?Lang=E>.
- [113] E. Fuentes, L. Arce, and J. Salom, “A review of domestic hot water consumption profiles for application in systems and buildings energy performance analysis,” *Renew. Sustain. Energy Rev.*, vol. 81, pp. 1530–1547, Jan. 2018, doi: 10.1016/J.RSER.2017.05.229.
- [114] S. Edwards, I. Beausoleil-Morrison, and A. Laperrière, “Representative hot water draw profiles at high temporal resolution for simulating the performance of solar thermal systems,” *Sol. Energy*, vol. 111, pp. 43–52, Jan. 2015, doi: 10.1016/J.SOLENER.2014.10.026.
- [115] A. Ferrantelli, K. Ahmed, P. Pylsy, and J. Kurnitski, “Analytical modelling and prediction formulas for domestic hot water consumption in residential Finnish apartments,” *Energy Build.*, vol. 143, pp. 53–60, May 2017, doi: 10.1016/j.enbuild.2017.03.021.
- [116] Water Research Foundation, “Residential End Uses of Water, Version 2,” p. 16, 2016, [Online]. Available: [www.waterrf.org/4309](http://www.waterrf.org/4309).
- [117] M. H. Nehrir, R. Jia, D. A. Pierre, and D. J. Hammerstrom, “Power Management of Aggregate Electric Water Heater Loads by Voltage Control,” in *2007 IEEE Power Engineering Society General Meeting*, Jun. 2007, pp. 1–6, doi: 10.1109/PES.2007.386024.
- [118] E. O’Dwyer, L. De Tommasi, K. Kouramas, M. Cychowski, and G. Lightbody, “Modelling and disturbance estimation for model predictive control in building heating systems,” *Energy Build.*, vol. 130, pp. 532–545, Oct. 2016, doi: 10.1016/J.ENBUILD.2016.08.077.
- [119] OpenLearn, “Calculating the heat loss of a house,” *Energy Build. - OpenLearn - Open Univ.*, [Online]. Available: <https://www.open.edu/openlearn/nature-environment/the-environment/energy-buildings/content-section-2.4.1>.
- [120] N. R. C. of Canada, *National Building Code of Canada, 2015*. National Research Council Canada, 2015.
- [121] A. M. Syed, “Electric thermal storage option for nova scotia power customers: A case study of a typical electrically heated nova scotia house,” *Energy Eng. J. Assoc. Energy Eng.*, vol. 108, no. 6, pp. 69–79, 2011, doi:

10.1080/01998595.2011.10412169.

- [122] S. Corporation, "Owner's and Installer's Manual for Room Heating Units-2100 Series." [Online]. Available: <https://www.steffes.com/>.
- [123] K. Ibrahim Elamari and K. I. Elamari, "Using electric water heaters (EWHs) for power balancing and frequency control in PV-Diesel Hybrid mini-grids," Concordia University, 2011.

## **Curriculum Vitae**

Candidate's full name: Manuel Arturo Mendoza Miranda

Universities attended (with dates and degrees obtained):

- University of New Brunswick (September 2019 to Present, Master of Science, Electrical Engineering)
- Universidad Central "Marta Abreu" de Las Villas (September 2012 – July 2017, Bachelor of Science, Telecommunications and Electronics)